ETANKFIRE – Experimental results of large ethanol fuel pool fires

Johan Sjöström, Glenn Appel,
Francine Amon, Henry Persson

SP Technical Research Institute of Sweden

Fire Research

SP Report 2015:12

ETANKFIRE – Experimental results of large ethanol fuel pool fires

Johan Sjöström, Glenn Appel,
Francine Amon, Henry Persson

Abstract

The intention of the tests conducted in this part of the ETANKFIRE project has been to investigate the burning behavior of various ethanol fuel mixtures. Two series of free-burning tests with ethanol fuel mixtures have been conducted, one in laboratory scale with a pool area of 2.0 m^2 and one in large scale with a pool area of 254 m^2. In both test series the burning rate, flame height and heat flux as a function of distance from the fires were measured and the effect of these parameters on the size of the fire area was investigated.

Two fuel mixtures were used in the large scale tests, E97 (97 % ethanol denatured with 3 % gasoline) and commercial E85 (85 % ethanol with 15 % gasoline). As no tests were made with "pure" gasoline in large scale, the measurements from E97 and E85 have been compared with calculated data and some previous experimental data from large scale gasoline fire tests.

The laboratory scale tests showed increasing heat flux with increasing proportion of gasoline in the fuel. However, for the large scale tests, the E97 and E85 fuels emitted the same radiant heat. In addition, the heat exposure towards the nearby surrounding is approximately 2-3 times higher for both the E97 and E85 fuels compared to calculated and experimental data on gasoline. The difference declines with increasing distance but is still about a factor 2 higher at distances of 30 - 40 m. The radiative fraction (ratio of radiant to chemical heat release) as a function of the fire area will probably have a larger influence on E85 compared to E97 due to the higher content of gasoline. Therefore, it is likely that a larger E97 fire would generate a higher heat flux compared to a similar E85 fire and the difference between the two would increase as the fire area increases.

This report comprise most of the experimental results given in the non-public report ETANKFIRE – Large scale burning behavior of ethanol fuels, SP Report 2013:02. Most of the time-resolved data is removed as well as some of the appendixes.

Key words: Ethanol, E85, E97, large scale fire tests, heat flux measurement, burning rate, radiative fraction, pool fire, alcohol, fire suppression

SP Sveriges Tekniska Forskningsinstitut
SP Technical Research Institute of Sweden

SP Report 2015:12
ISBN 978-91-88001-42-9
ISSN 0284-5172
Borås 2015

Contents

Preface

The use of ethanol has increased significantly as a means to fulfill climate goals by replacing fossil fuels with renewable fuels, but the introduction of ethanol fuels creates new risks and challenges from a fire protection point of view. SP Fire Technology, together with the Swedish Petroleum and Biofuel Institute (SPBI), took the initiative to develop a proposal for a joint industry research project on ethanol tank fire fighting – ETANKFIRE. The project will provide a platform of knowledge ensuring proper investment in fire protection of ethanol storage facilities. The goals of the project are to develop and validate a methodology for fire protection and suppression of storage tank fires containing ethanol fuels and to determine the large scale burning behavior of ethanol fuels.

The ETANKFIRE project is structured into seven work packages (WP0 to WP6) as shown below. The work in WP1 to WP4 will be related to the extinguishment of ethanol storage tank fires while work related to the burning behavior has been handled in WP5. The project is divided in two phases and Phase 1 includes WP1, WP2 and WP5. Phase 2, focusing on WP3 and WP4, is not planned to be launched until the work in Phase 1 is completed and necessary funding has been obtained

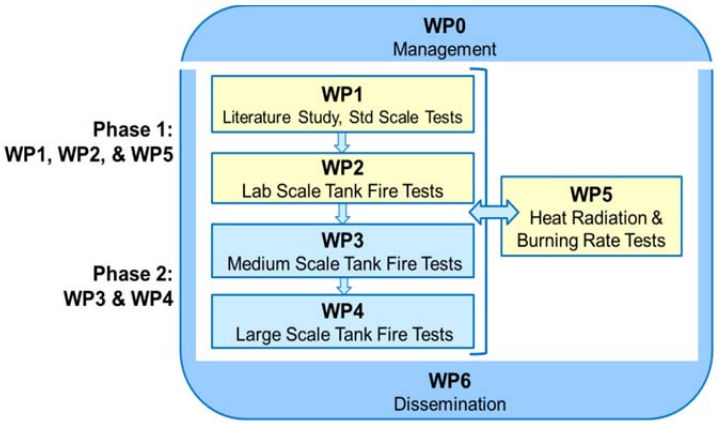

ETANKFIRE project structure where Phase 1 involves WP1, WP2 and WP5 and Phase 2 is planned to focus on WP3 and WP4 when Phase 1 is completed. The activities in WP0 and WP6 will be included in both Phase 1 and Phase 2.

At the time of conducting the tests in WP5 which are reported here, the ETANKFIRE consortium had the following Full Partners and Observer Members which are gratefully acknowledged for their contribution.

- BRANDFORSK (Swedish Fire Research Board) funding through project 603-111
- Släckmedelscentralen SMC AB, a subsidiary company to the SPBI (Swedish Petroleum and Biofuel Institute)
- Lantmännen ek. för, Swedish ethanol producer
- Shell Research Limited (Observer Member)

The testing and research group (RT Group), responsible for the experimental work and the project management consists of:

- SP Technical Research Institute of Sweden - Department of Fire Technology
- Resource Protection International, UK

Extended summary

The intention of the tests conducted within this part of the ETANKFIRE project has been to investigate the burning behavior of various ethanol fuel mixtures and how these parameters relate to the size of the fire area.

During a risk analysis for a fuel processing plant or storage facility, commercial software is normally used to evaluate a set of fire scenarios relevant to the facility and to calculate impact of the fire, e.g. the incident heat flux towards nearby objects and firefighting personnel. However, most models are developed and to some extent validated for petroleum products while large scale experimental data on ethanol fuels is lacking completely.

To provide experimental data that could be used for comparison and validation of models used to describe the fire, two series of free-burning tests with ethanol fuel mixtures have been conducted, one in laboratory scale with a pool area of 2.0 m^2 and one in large scale with a pool area of 254 m^2. In both test series the burning rate, flame height and heat flux as a function of distance from the fires were measured and the effect of these parameters on the size of the fire area was investigated. The laboratory scale tests were performed to verify the measuring technique to be used in the large scale tests, and also to provide comparable data to better understand the influence of test scale. However, the main focus of the project has been on the large scale tests in order to provide model validation data from a "real scale fire". Two fuel mixtures were used in the large scale tests, E97 (97 % ethanol denatured with 3% gasoline) and commercial E85 (85 % ethanol with 15 % gasoline). In addition, a fuel mixture of E50 (50 % ethanol with 50 % gasoline) was used in the laboratory scale tests. As no tests were made with "pure" gasoline, the measurements from E97 and E85 have been compared with calculated data[1] and some previous experimental data from large scale tests [1, 2].

The results from the two test series clearly show differences in burning behavior between the various fuel mixtures and the influence of the size of the fire. In laboratory scale, the heat flux is lowest for E97 and increases as the proportion of gasoline increases, from 4.5 kW/m^2 for E97 to 5.5 kW/m^2 for E85 and 7.0 kW/m^2 for E50 at a distance of 3 m from the pool rim. Previous measurements at a similar scale show that pure gasoline gives a corresponding heat flux of about 9 kW/m^2 [3]. Laboratory scale heat flux results are shown in the figure below for 1 m and 3 m from the pool rim.

[1] Calculated using Process Hazard Analysis Sofware Tool (PHAST) and Shell Fire, Release, Explosion, Dispersion hazard consequence modelling package (FRED).

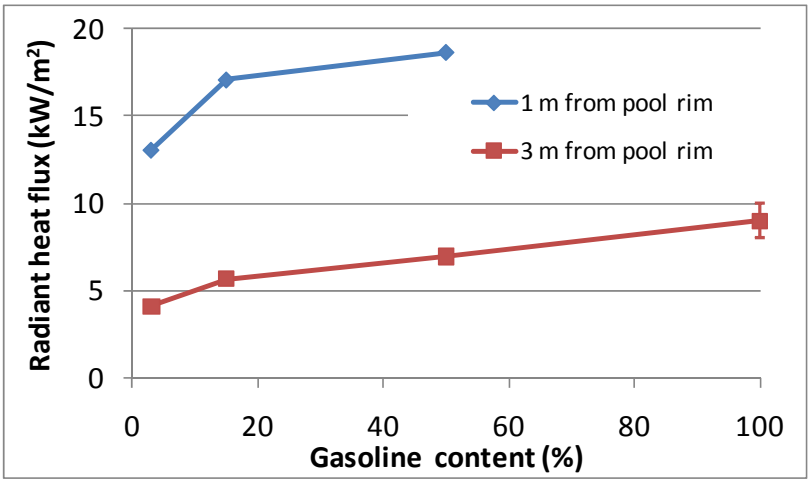

Radiant heat flux (average over ten minutes) from laboratory scale (2.0 m^2 pool area), 1 and 3 m from pool rim. Data for gasoline is estimated from previous tests.

In contrast to the laboratory scale tests, there was virtually no difference between the average measured heat flux from E97 and E85 in the large scale tests. The figure below shows surface temperatures of plate thermometers as a function of distance from the pool rim. There are several reasons for the differences in burning behavior resulting from changing the scale of the fire tests:

- The combustion becomes less complete for fuels with longer hydrocarbon chains. As the pool size is increased the central part of the pool fire becomes more oxygen deprived, leading to incomplete combustion and more smoke production. This is particularly evident for longer-chain hydrocarbon mixes such as gasoline, which are more prone to produce smoke compared to short-chain alcohols such as ethanol [2, 4].
- A substantial portion of flames from large pools of hydrocarbon fuels can be obscured by smoke that covers the outer parts of the flame. The smoke absorbs radiation from the hot flames. A larger portion of gasoline increases the smoke production, which produces a larger effect for E85 compared to E97. In these experiments a higher smoke production from E85 was clearly apparent compared to E97 [5]. Thus, the increased smoke production balances the higher heating value of combustion of E85 compared to E97.
- For a small flame, the flame emissivity of a short-chain alcohol could be substantially reduced compared to gasoline while the emissivity is close to 1.0 for both fuels in large scale [6].

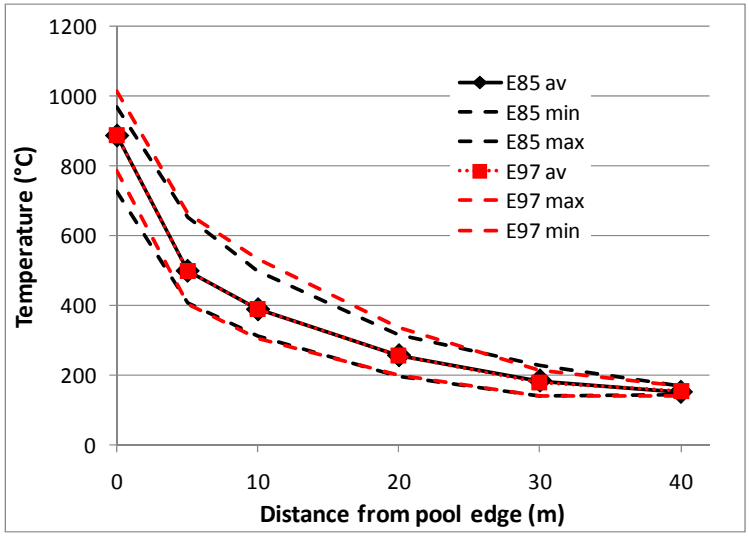

Comparison of temperatures of plate thermometers facing the E97 and E85 fires in large scale. The upper and lower curves in the diagram represent the measured maximum and minimum values.

The pool size dependence of burning rate and radiant fraction have been studied for many hydrocarbon fuels [2]. The burning rate (regression of fuel surface) increases with pool size for small pool areas before it saturates to a constant value. This means that the evaporation rate, as mass per unit time, increases proportionally to pool area for large pools. Despite this, the exposure by heat radiation towards the surroundings of the fire does not follow the same increasing pattern. Thus, the ratio of heat being radiated from the flame to the chemical heat release rate (theoretical heat release rate from complete combustion of all evaporated fuel) decreases rapidly with increasing pool size.

The figure below shows the typical radiative fraction for gasoline and other hydrocarbon fuels as a function of pool size. For small pool sizes it is around 30 % to 50 % but decreases significantly above pool diameters of ~2 m and is about 5 - 10 % for pool diameters of 20 m.

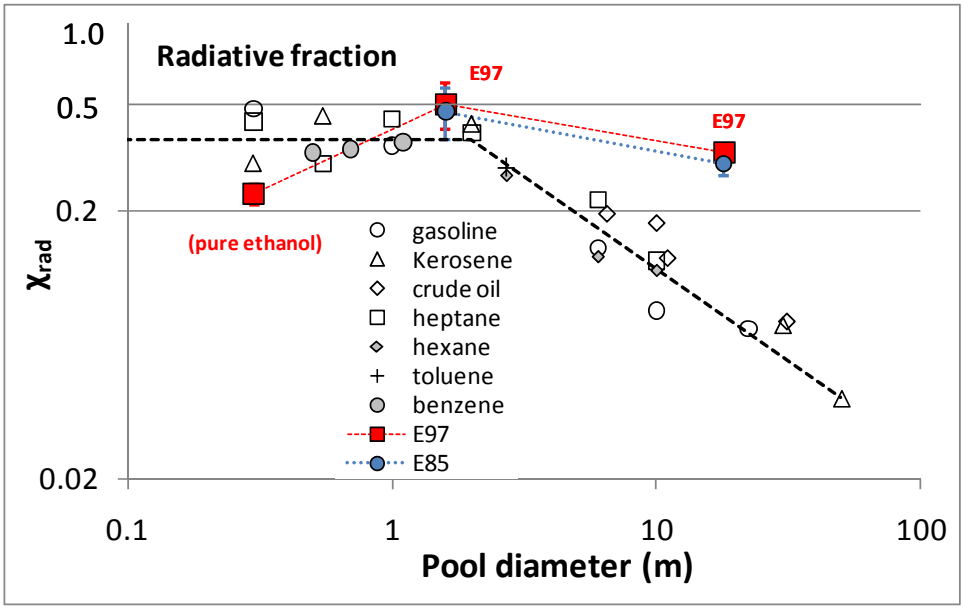

Radiative fraction (radiative heat release divided by total heat release for a complete combustion) versus pool size.

However, based on the large scale test results from this study, it is obvious that E97 and E85 does not behave in the same way. As the radiative fraction of hydrocarbon fuels significantly decreases the corresponding decrease for ethanol is much less. This is the most important reason why large scale burning behavior of alcohols cannot be based on hydrocarbon test results or laboratory scale experiments.

The consequence of these differences in large scale situations becomes very obvious when the heat flux data from the large scale ethanol tests are compared to gasoline. Below is a comparison between the E97 test results and calculated results for gasoline using two different software packages, Phast and FRED, perpendicular to the wind direction. Also some results from previous, similar large scale fire tests are included.

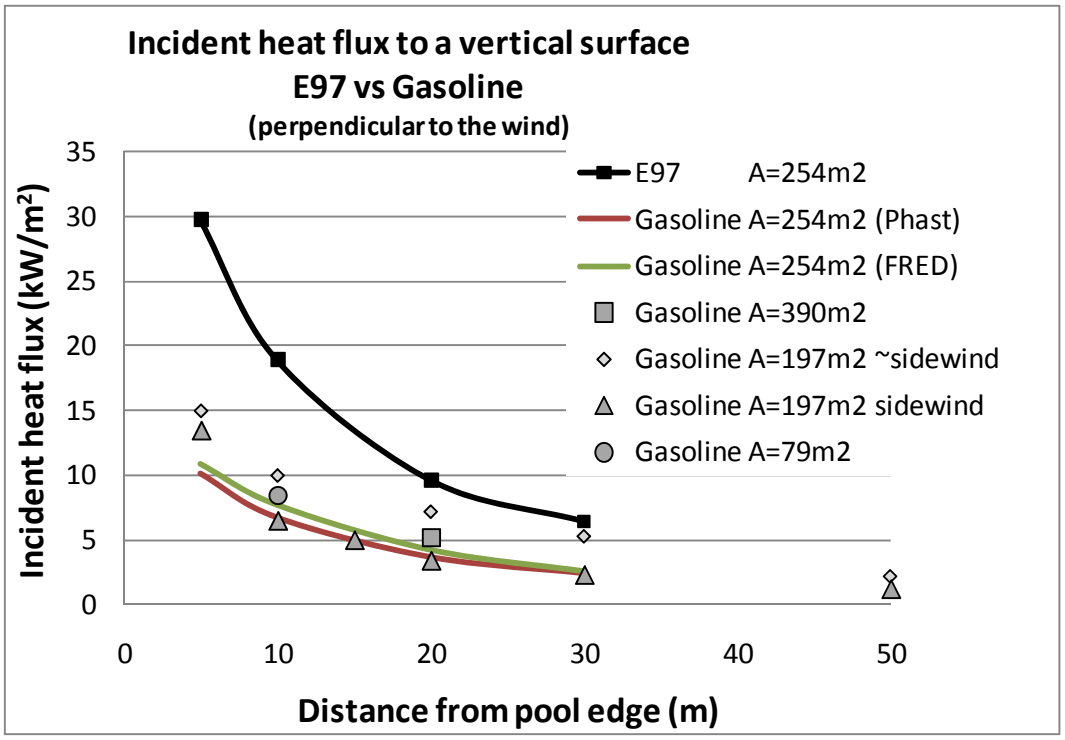

Measured heat flux perpendicular to the wind direction for E97 compared to calculated and experimental data for gasoline [1, 2].

The large scale results show that the heat exposure towards the nearby surroundings (within 5 m) is on the order of 3 times higher for the E97 and E85 fuel compared to calculated and experimental data for gasoline. The difference decreases with distance from the pool rim but is still in the order of a factor 2 higher at 30-40 m. The large scale tests showed only minor differences between E85 and E97 so the comparion is also valid for E85 in this scale.

These differences are influenced by the size of the fire and are only relevant for the fire area (about 250 m^2) used in these tests. If the fire area increases, the difference between gasoline and E97 would probably increase because the radiative fraction from the E97 fire appears to be only slightly influenced by the fire area while the radiative fraction for gasoline is significantly reduced as the fire area increases.

In these tests, the heat flux generated by the E97 and E85 fires was almost the same. The radiative fraction as a function of fire area will probably have a larger influence on E85 compared to E97 due to the higher content of gasoline, so it is likely that a larger E97 fire

would generate a higher heat flux compared to a similar E85 fire and the difference between the two would increase with increasing fire area.

In order to estimate the heat exposure from fires under various conditions, and thereby be able to judge the consequences in a real industrial environment, software like Phast and FRED are needed. However, in order to obtain reliable results, it is important that differences in fire behavior between fuel types is considered, such as the differences between ethanol and gasoline observed in these tests.

1 Introduction and background

1.1 Ethanol use and storage hazards

The use of ethanol has increased significantly as a means to fulfill climate goals by replacing fossil fuels with renewable fuels. In the 2007 Spring Council, the EU agreed on targets to cut greenhouse gas emissions by at least 20 % until 2020. To have a real impact on the green economy and reach the emission targets it is essential to successfully introduce a broad biobased economy, including ethanol fuels as one component.

The main use of ethanol is for low blending in gasoline, but it is also used as E85 and "diesel ethanol". In 2011, the acceptable proportion of ethanol in low blended fuels was increased from 5 % to 10 % in Europe. Similarly, in the US the use of ethanol fuels has increased dramatically during the last decade. Presently (2012) the ethanol content in the gasoline sold in the US is nominally 10 % but in some states, the ethanol content has been increased to 15 %.

The obvious consequence of increasing the volume of low blended ethanol, both in Europe and the US is that the volume of bulk ethanol transported, handled and stored will increase dramatically in coming years. The diameter/volume of the storage tanks is also increasing, making a fire and ensuing firefighting operations a significant challenge. However, experience in fighting storage tank fires involving ethanol or other water miscible fuels is very limited and those few tank fires that have occurred have resulted in burn out rather than extinguishment [7-10].

A very important and related issue is that the burning behavior of a large scale ethanol fire may be significantly different from that of a petroleum fire. Previous tests with similar fuels indicate that the heat flux from an ethanol fire could be significantly higher than that of a gasoline fire, which increases the risks for fire escalation and the need for improved fire protection.

Although tank fires in general are rare, and the number of ethanol tank fires to date is very few, extensive fire protection measures will, as for other flammable liquids, be required based on various national laws and regulations. Typically this translates into significant investments, both in preventative measures and risk mitigation measures including extinguishment in the case of a full scale fire. However, as practical experience is very limited and the standards for fire protection often lack specific information concerning ethanol and similar fuels, there is a great risk that such investments will not provide the fire protection level as expected by the regulators.

Therefore, the main goal of the ETANKFIRE project is to provide a platform of knowledge ensuring proper investment in the fire protection of ethanol storage facilities. This will involve understanding large scale burning behaviour, and developing and validating a methodology for fighting fires in tanks containing ethanol fuels. This report relates to free-burning tests conducted within this project.

1.2 Burning behavior of ethanol fuels

The intent of study is to determine the burning behavior of ethanol fuels under large scale conditions. Ethanol typically burns more efficiently than gasoline; for large scale fires this difference is potentially significant. The issue is further complicated by the fact that the size of the fire has an impact on the burning behavior of the fuel. Experience from various laboratory scale fires shows that heat flux is lower from an ethanol fire compared to gasoline. However, there are indications that the opposite behavior may be true in a large scale fire based on observations made during a series of fire tests conducted on a 200 m^2 mixture of 70 % acetone and 30 % ethanol [1]. Measurements indicated that the heat flux from the acetone/ethanol fire was about twice that of gasoline in this scale, although gasoline produced significantly higher heat flux in laboratory scale tests. The reason for this difference is probably that as the scale increases, gasoline fires generate increasingly larger amounts of smoke which tend to block the visible parts of the flames, thereby reducing the heat flux. An acetone/ethanol fire is almost free from smoke and the associated heat flux is, therefore, not dissipated by smoke. This could imply that the heat flux from an ethanol fuel fire will exceed that of a gasoline fire in larger scale fires, with the difference increasing as the scale increases.

There are several commercial computer programs for the calculation of heat exposure from pool fires and tank fires, but validation based on large scale experimental data is lacking. The calculated results might differ significantly between various programs depending on the assumptions made for ethanol fuels in the program code or by the user of the program. Hence, large scale test data is crucial to validate such computer models, thereby improving our ability to make reliable risk assessments without the need for full scale testing in the future.

The intention of the tests reported here was to make accurate measurements of burning rate, flame height and heat flux as a function of distance from the fire in at least three directions (upwind, downwind and crosswind). The main tests were focused on large scale conditions. Some pre-tests were made in laboratory scale to obtain results on burning rate and to verify the measuring technique, which was used for the final planning of the large scale tests. The laboratory scale results are also valuable for understanding the influence of the scale factor on radiated heat and burning rate.

2 Measurement techniques

A description of the instrumentation and measurement techniques used for both the laboratory scale and the large scale experiments is provided in the following sections.

2.1 Plate thermometers

In order to measure the heat exposure from the fire, the temperature at different distances from the fire has been recorded by using plate thermometers (PT). Based on these temperature measurements, the heat flux at each position can be calculated using the calculation method described below.

In these tests, a newly designed plate thermometer was used, designated as “insulated Plate Thermometer”. The intention with the design of the insulated PT was to provide a simple, reliable and robust instrument for measurement of heat flux in e.g. field test conditions compared to the use of traditional heat flux meters (see chapter 2.2). Compared to the “standard Plate Thermometer” defined for furnace control of fire resistance tests according to ISO 834 [11], the insulated PT has improved insulation on the back side of the steel plate, see Figure 1. This is to reduce the thermal losses when it is used in ambient temperature conditions. The standard PT is mainly used in furnaces or close to objects exposed to direct flames or very high temperatures. In these conditions, the ambient temperature and the radiative temperature is within the same order of magnitude, making the heat loss less significant. In order to improve the response time, the insulated PT has also a thinner steel plate on the front side compared to the standard PT.

Note: In this report, the abbreviation PT will be used in the text (both for singular and plural cases) and it refers to the insulated PT unless specifically mentioned otherwise.

The insulated PT has also the advantage of providing a surface temperature. This temperature is close to the maximum surface temperature that an object would obtain at a certain heat exposure. In practice, most exposed object will obtain a lower temperature because the thermal inertia (product of thermal conductivity, density and heat capacity) is larger for most other objects compared to the insulated PT. Thus, the heat conduction into the object, the higher heat capacity and the lower emissivity of most other materials ensures a safety margin when using insulated PT temperature measurements. The true temperature of an object can be calculated using insulated PT measurement data and heat transfer calculations.

Note that the high temperature of the PT does not yield “maximum” values for the incident radiant heat flux, which is calculated based on the specific properties of the PT. Thus, the PT measurements enables us to calculate true incident heat fluxes just as those measured by a water cooled heat flux meter [12, 13].

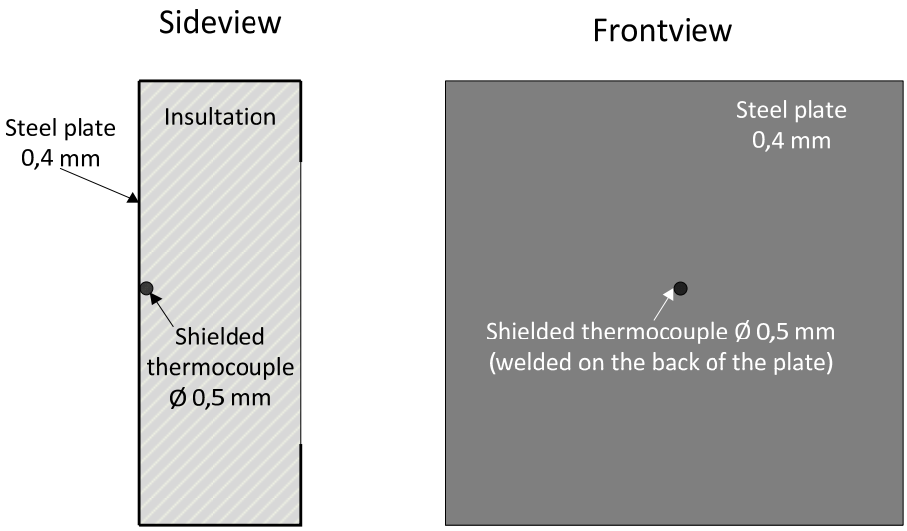

Figure 1 **Schematic sketch of the plate thermometer (100 by 100 by 30 mm). Shown in the figure is the steel plate, the insulation and the measuring point, in the center of the plate facing the fire.**

The basic elements of the insulated PT are a thin steel plate, a 0.5 mm shielded thermocouple type K welded onto the inside of the steel plate, and insulation. The steel plate (Inconel600) has a thickness of 0.4 mm compared to 0.7 mm for the standard PT. The insulation thickness is 30 mm, compared to 10 mm for the standard PT. A photo of the test set up for the laboratory scale tests is shown in Figure 2. This arrangement was also used for the full scale tests.

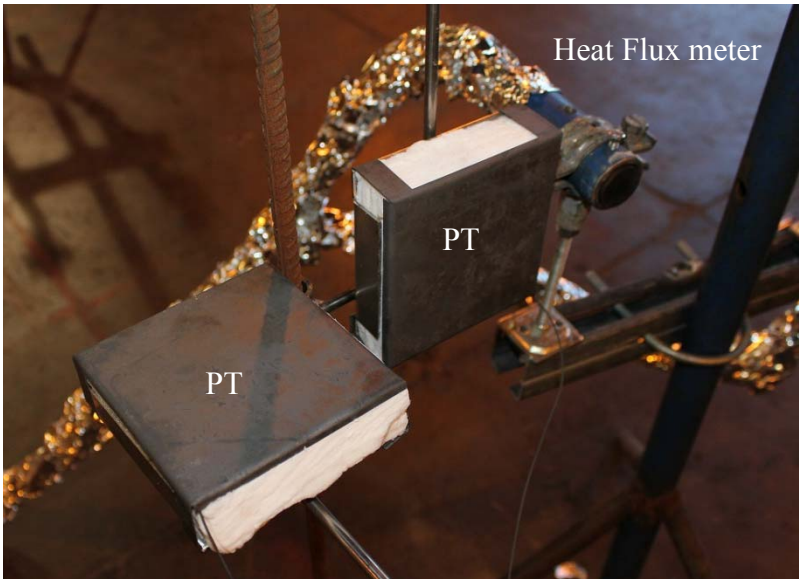

Figure 2 **A picture of the insulated PT used during the tests. A traditional heat flux meter is seen to the right of the vertical PT.**

As previously mentioned, one main advantage with the PT is that it can be used for accurate heat flux measurements. The method of using PT measurements to calculate radiant heat flux is based on the study by Ingason and Wickström [12]. This method has been refined and is more robust using the insulated PTs with thicker insulation and less overlap of metal in its construction. The model takes into account incident and emitted heat flux, convective heat transfer at the plate surface, combined energy losses through

conduction and convection at the back side as well as energy storage due to heating of the metal and insulation. The incident radiant heat flux, $\dot{q}''_{inc}$, is calculated through equation 1:

$$\dot{q}''_{inc} = \sigma T_{PT}^4 + \frac{(h+K_{PT})(T_{PT}-T_\infty)+C_{PT}\frac{dT_{PT}}{dt}}{\varepsilon_{PT}}. \quad (1)$$

where T_{PT} and T_∞ are temperatures of PT and ambient air, respectively, ε_{PT} is plate emissivity, K_{PT} is the loss correction factor (4 W/m^{2}K for the insulated PT) and C_{PT} is the storage correction factor due to the heat capacity of the insulated PT (3000 J/m^{2}K). The storage correction factor compensates for the finite time constant of the insulated PT. h is the convective heat transfer coefficient calculated through equation 2 [13]:

$$h = 1.9T_\infty^{0.087}\sqrt{\frac{u_\infty}{x}} \quad (2)$$

where u_∞ is air velocity and x is size of the PT.

To reduce errors and scattered results, the derivative in equation 1 is a floating point central difference using time steps of ± 20 seconds. Further information about the accuracy of this method is presented by Häggkvist, et.al.[14].

2.2 Heat flux meters

Heat flux meters [15] were used to measure the heat radiated from the fires and to validate the measurements taken with the PT. In general, heat flux meters have a well-characterized sensing surface that responds to radiation coming from a heat source and converts it to a voltage. The heat flux meters used in these tests were water cooled and look similar to Figure 3. The heat flux meters used have a nominal range of 0 - 50 kW/m^2 and 0 – 20 kW/m^2, respectively. In the laboratory scale tests, two heat flux meters were placed 1 m from the rim of the fire, facing each other as shown in Figure 7. In the large scale tests, they were placed at 5, 10 and 30 m distances from the rim of the fire as shown in Figure 11. The heat flux meters used for the laboratory scale tests had been calibrated according to ISO 14934-2 within one year prior to the testing and the heat flux meters used for the large scale tests were calibrated after the testing was complete.

The heat flux meters used for these tests were ruggedized by mounting them in steel tubes and wrapping insulation around the electrical connection and water tubes to protect them from extinguishing water and other hazards that may be encountered in a fire testing environment. A ruggedized heat flux meter is shown in Figure 2 on the far right.

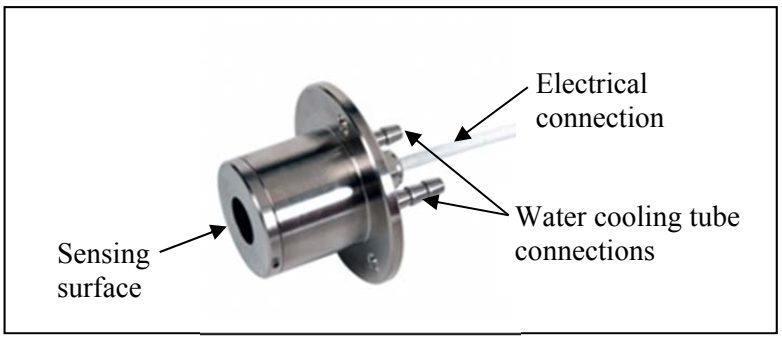

Figure 3 A typical heat flux meter

Heat flux meters are relatively accurate instruments for measuring radiated heat, have well-documented calibration methodology and measurement uncertainty[2]. They are recognized within the fire research community as being a reliable means of measuring the thermal impact of fire and are therefore they are widely used for fire testing. Heat flux meters also have a downside: they are expensive relative to PT, require cooling of water and they have a limited measurement range.

2.3 Burning rate measurements

To measure the burning rate of the fuel, a thermocouple tree was constructed and placed at the bottom in the center of the pool, see Figure 4.

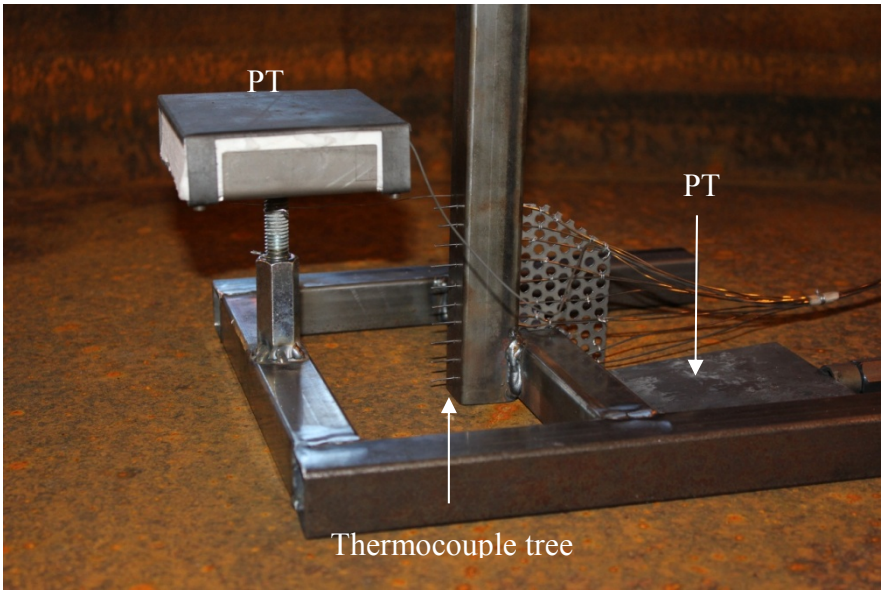

Figure 4 **Thermocouple tree arrangement (photo from laboratory scale tests). The photo also shows an insulated PT which was located just above the fuel surface and a standard PT which was placed on the bottom of the pool. In addition, a thermocouple for gas measurements was located just below the insulated PT (not visible on the photo).**

The thermocouple tree used 10 shielded, type K thermocouples with a diameter of 1 mm and a distance of 10 mm between. The thermocouple shield was long enough to reach beyond the rim of the fire pool.

At the start of the test, most of the thermocouples were submerged within the fuel layer, measuring the fuel temperature, which was also measured by the standard PT. As the fuel was consumed by the fire, one by one the thermocouples became exposed to combustion gases and flames just above the fuel surface resulting in a very sharp increase in temperature, see Figure 5. The burning rate was calculated by measuring the time between the sharp rise in each set of thermocouple measurements.

The PT above the fuel and at the bottom of the tray/pool were used to measure the thermal impact towards the fuel surface and the heat flux transmitted through the fuel to the bottom of the tray/pool, respectively, which could possibly cause an additional heating effect of the fuel from below.

[2] According to the manufacturer, the uncertainty of the output from the heat flux meters used in these tests is ± 3 % of the full measurement range.

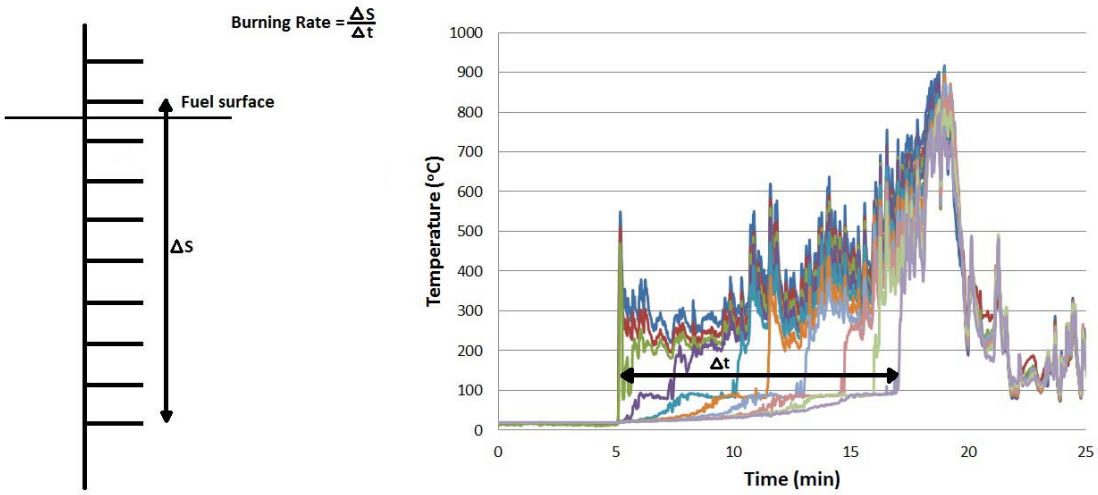

Figure 5 **An illustration of the principle for burning rate measurements and a typical temperature diagram obtained during a test. In the example, the fire was ignited at 5:00 min.**

2.4 Flame height measurements

Video cameras were used to estimate the flame height during the tests. Before each test, the camera settings were calibrated using a measuring stick having markings every 0.5 m, see Figure 6. The stick was placed in front of the camera lens at a distance equal to 1/10 of the distance to the pool center which means that each marking represented 5 m at the pool center. These markings have been edited into the original video recording making it possible to observe the flame height during the tests.

Figure 6 **A measuring stick with markings every 0.5 m located at 1/10 of the distance to the pool center was used as a reference for the flame height measurements. The superimposed markings on the flame in the left image are 5 m apart.**

In case the video lens (zoom) was adjusted during the tests the marking stick was recorded again after the test with the new lens setting, allowing the markings to be adjusted on the video accordingly.

The evaluation of flame height has been made from video captured by the camera located in the east direction because it was perpendicular to the main wind direction and thereby also provided a possibility to observe any flame inclination caused by the wind.

2.5 IR measurements

In addition to visible-spectrum video, the fire tests were also recorded using an infrared (IR) camera which converts radiation to temperature and thus provides a temperature profile of the flame. The camera was located close to the east video camera to provide a direct video comparison. For these comparisons the emissivity was set at 1.0. The measuring stick for flame height was also visible to the IR camera.

The IR camera used was a FLIR A320, recording temperatures between 80 and 1300 ºC at a frequency of four images per second. The camera operates in the 7.5 – 13 μm wavelength range, which is sensitive to radiated heat but also penetrates smoke much better than the visible wavelength band. The thermal sensitivity of the IR camera is 70 mK at 30 ^{o}C and generally becomes less sensitive at higher temperatures. This camera was located 57.5 m from the pool center, has a 320 by 240 (horizontal by vertical) detector containing 76800 pixels, and was fitted with a 45 degree lens, which means that each detector pixel viewed an area of approximately 18 by 18 cm.

2.6 Video recordings and documentation

In total, four video cameras were used to record the fire tests. Two cameras were located east of the fire at a distance of 57 m from the pool center, one camera 65 m northwest and one camera 50 m almost south from the pool center. In addition to the documentation captured by the video cameras as described above, photos were also taken using several digital cameras.

A weather station recording wind speed, wind direction, air humidity and air temperature was located about 50 m NNW of fire test pool at 4.5 m height (see also chapter 3.2.2).

3 Test configuration

Before the large scale free-burning tests were conducted, a series of pre-tests were made in laboratory scale to investigate the coupling between small and large scale testing as well as to verify the measuring technique. The measurement equipment described in chapter 2 was used in both test series, and below is a description of the test setups used for the laboratory scale and large scale tests.

3.1 Laboratory scale free-burning tests

3.1.1 Test set-up and instrumentation

The laboratory scale tests were performed in the large fire hall at SP Fire Technology in Borås. A steel pan having a diameter of 1.6 m corresponding to an area of 2.0 m^2 was used. The rim height of the pan was 250 mm. The pan was placed on a load cell platform and was positioned directly below an industrial calorimeter hood system.

In order to measure the heat flux from the fire, nine PT were located around the pool at 0 m, 1 m and 3 m distance from the rim of the pan, see Figure 7 and Figure 8. Five PT were mounted vertically (facing the fire) and three were mounted horizontally (facing upwards). In addition to the PT, two heat flux meters were also used, both facing the fire, in order to provide a comparison between the two instruments. The horizontal and vertical orientation of the PT enables a calculation of the incident radiant heat flux to a surface in any orientation.

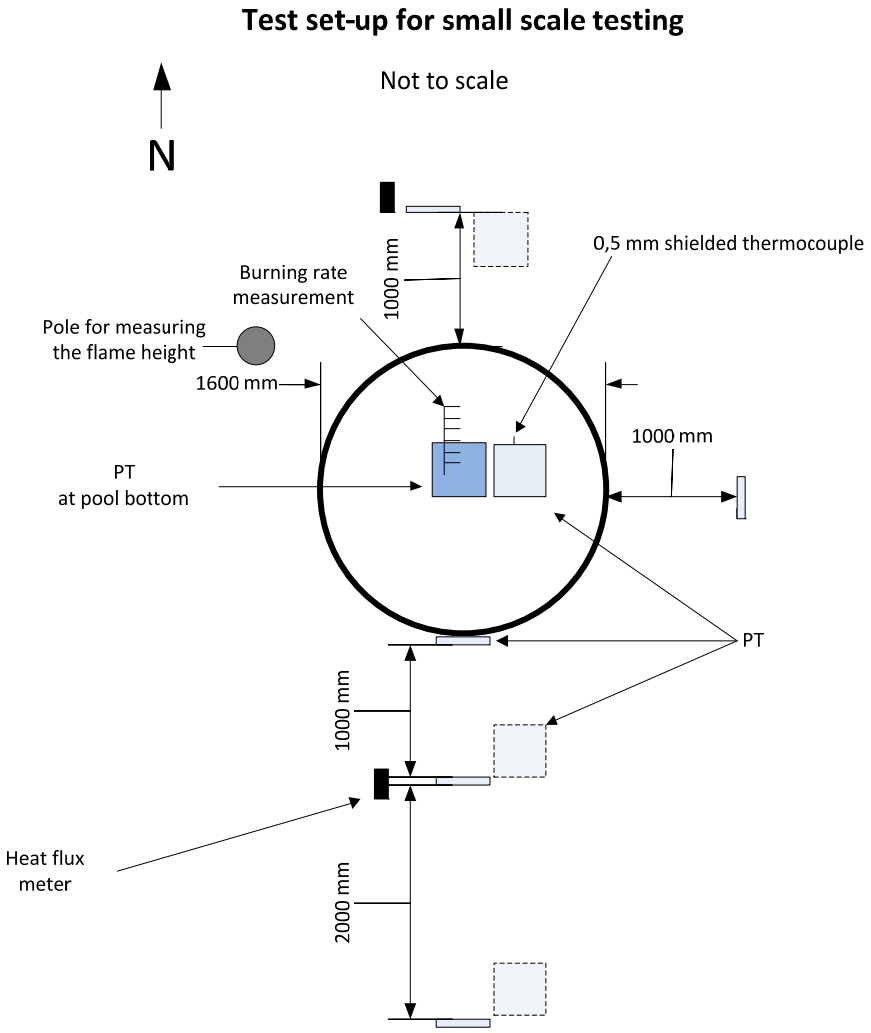

Figure 7 **Configuration of the measuring equipment during the laboratory scale free-burning tests (not to scale). The PT on the pool bottom and the PT to east of the pool were standard PT, the rest were insulated PT.**

The burning rate and the temperature conditions inside the flame were measured using the thermocouple arrangement described in chapter 2.3, which was located in the center of the pool. As a complement to the burning rate measurements using the thermocouple tree, the weight loss was also recorded by the load cell, providing a possibility to compare the results.

The flame height was measured by placing a measuring pole beside the pool with markings every meter.

Figure 8 **The 2.0 m^2 fire tray with the thermocouple arrangement in the tray and the PT and heat flux meter in "south" direction.**

3.1.2 Fuel qualities

Three different fuels were used for the laboratory scale tests: E97, E85 and E50. Further information about the reason for the selection of these qualities is provided in chapter 3.2.3.

For each test, approximately 200 litres of fuel was used, corresponding to a nominal fuel depth of 100 mm. The E85 fuel was a commercial (summer) quality purchased at a local petrol station. The E97 and the E50 qualities were prepared by mixing ethanol (purity 99.8 %, delivered from Lantmännen) and 98 octane commercial gasoline purchased at a local petrol station. As the commercial gasoline already contain 5 % of ethanol, a compensation was made during mixing to obtain the intended concentration. The mixing of ethanol/gasoline was made according to Table 1.

Table 1 **The proportion of ethanol (in liters) and gasoline used during the tests. The E85 was a commercial quality and was not mixed.**

	E97	E85	E50
Gasoline	6,4		110,4
E85		198,5	
Ethanol	193,6		99,0

3.2 Large scale free-burning tests

3.2.1 Test location and fire test pool

The large scale fire tests were conducted at the Dala Mitt Fire Brigade training center in Borlänge, Sweden. An existing concrete pool having a diameter of 24 m forms the base for the test pool. As the existing pool bottom was bowl shaped with a maximum depth about 0.4 m in the center of the pool, the pool had to be modified to provide a defined fire area and a constant fuel depth. The existing pool was therefore filled with a new layer of concrete forming a flat surface. To provide the containment for the fuel, a 150 mm high rim having an internal diameter of 18 m (creating a surface area of 254.3 m^2) was molded in concrete together with the new concrete surface, see Figure 9 and Figure 10. The concrete mixture contained polypropylene and steel fibers to reduce spalling from the concrete during the later stage of the fire test when the fuel layer became very thin and the concrete was exposed to full heat flux from the flames.

Figure 9 **The fire tests were performed on an existing fire test pool (Ø = 24 m) made of concrete and with a varying depth. An inner pool with a diameter of 18 m was constructed to provide a defined test area and a constant fuel depth. The rim of the inner pool was 150 mm high. The pipe to the lower right was used to fill the pool with fuel.**

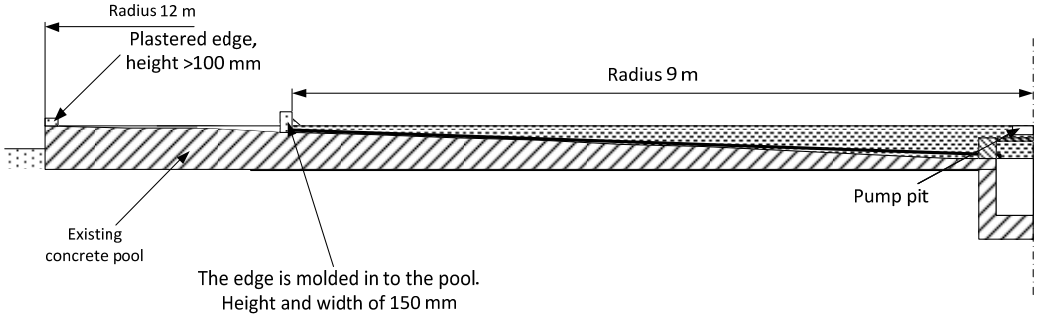

Figure 10 **A cross section (half symmetry) of the original concrete pool and the new modified fire test pool.**

3.2.2 Test set-up and instrumentation

The PT used for heat flux measurements described in chapter 2.1 were located in four directions (north, east, south and west) around the fire test pool, see Figure 11. The closest PT were located at the rim of the pool and exposed directly to the flames. The other PT were located at 5 m, 10 m, 20 m and 30 m from the rim of the pool. In the north (downwind) direction, there was an additional PT located at 40 m. All PT were mounted on an adjustable stand so that they were all at the same level as the rim of the fire test pool; due to the slope of the surrounding ground, this corresponded to a height of about 0.5 m – 1.4 m above the ground.

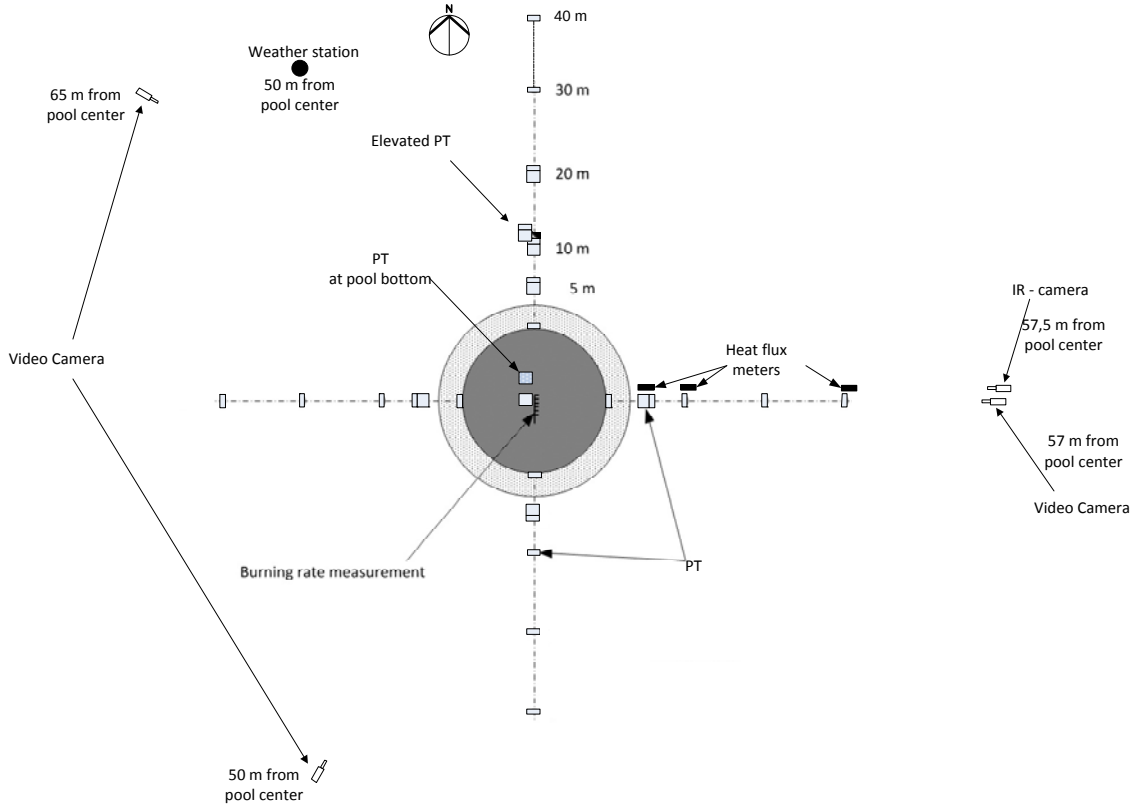

Figure 11 Configuration of the measuring equipment during the large scale free-burning tests. Instrumentation was located in all four directions and in the pool center. In both tests, the wind was predominantly blowing from south. The PT at the pool bottom is a standard PT, the rest are insulated PT.

Most of the PT were located in a vertical orientation (with the measuring surface facing the flame) to record the horizontal heat flux distribution. However, at some locations (5 m in all directions, as well as 10 and 20 m north), an additional PT was positioned horizontally (facing the sky) beside the other PT. At 10 m north, two PT were elevated to a height of 5.5 m above the main instrumentation (6.1 m above ground level), and mounted in two different directions, one facing the fire and one facing the sky. This was to study the influence of exposure at various heights in the downwind direction, e.g. the exposure to a nearby tank wall/tank roof.

In order to provide a comparison to the heat flux measured using the PT, three heat flux meters were located beside the PT at 5 m, 10 m and 30 m in the east direction, see Figure 12.

The burning rate and the flame temperature conditions inside the flame were measured using the thermocouple tree arrangement described in chapter 2.3, which was placed in the center of the pool.

The video cameras were located east, southwest, and northwest of the fire. The IR-camera was located next to the video camera east of the fire, see Figure 14.

Figure 12 **A picture of the measuring station (5 m east of the fire) where PT were mounted both in horizontal and vertical orientation, This station also included a heat flux meter.**

Figure 13 **A view of the measurement setup in the west direction with the closest PT mounted on the rim of the test pool.**

Figure 14 **The location of two video cameras, one digital camera and one IR-camera at 57 m (IR 57.5 m) from the pool center in east direction.**

3.2.3 Fuel qualities

Two different fuels were used in the large scale tests, E97 and E85. The E97 was ethanol denatured with 3 % gasoline. As all ethanol stored in tanks at fuel depots (in Sweden) must be denaturized for tax reasons, E97 is the product that is commonly stored in ethanol tanks before mixing to commercial fuel qualities. The specific E97 fuel used in the test contained 3.3 %-vol (3.1 %-weight) of gasoline.

E85 is the commercial fuel quality used for flexi fuel cars. The nominal mixture is 85 % ethanol and 15 % gasoline (by volume), but variations are allowed, e.g. there are different qualities for winter or summer conditions. The allowed range of mixture according to the standard (SS 155480:2012) is 75 % - 86 % ethanol (summer quality) and the remaining part gasoline. In these tests, a summer quality of E85 was used. The specific E85 fuel used in the test contained 15 % gasoline.

In both tests, the fuel quantity was about 20 000 L of fuel. This gives a nominal depth of approximately 80 mm throughout the entire pool (given that the pool is perfectly flat). In both tests, the fuel was allowed to burn out completely.

Note: The E50-quality, as was used in the laboratory scale tests was not included in large scale due to budget restrictions. E50 is not a fuel quality normally handled or stored at fuel depots, but running a large scale test with E50 (had enough funding been available) would have provided an opportunity for a better understanding of the influence of different fuel mixtures.

4 Results

A summary of the most important results from the two test series is presented in the following sections.

4.1 Laboratory scale tests

The laboratory scale free-burning tests show a significant difference between the three different fuel mixtures and in Figure 15 a photo from each of the fuels is shown.

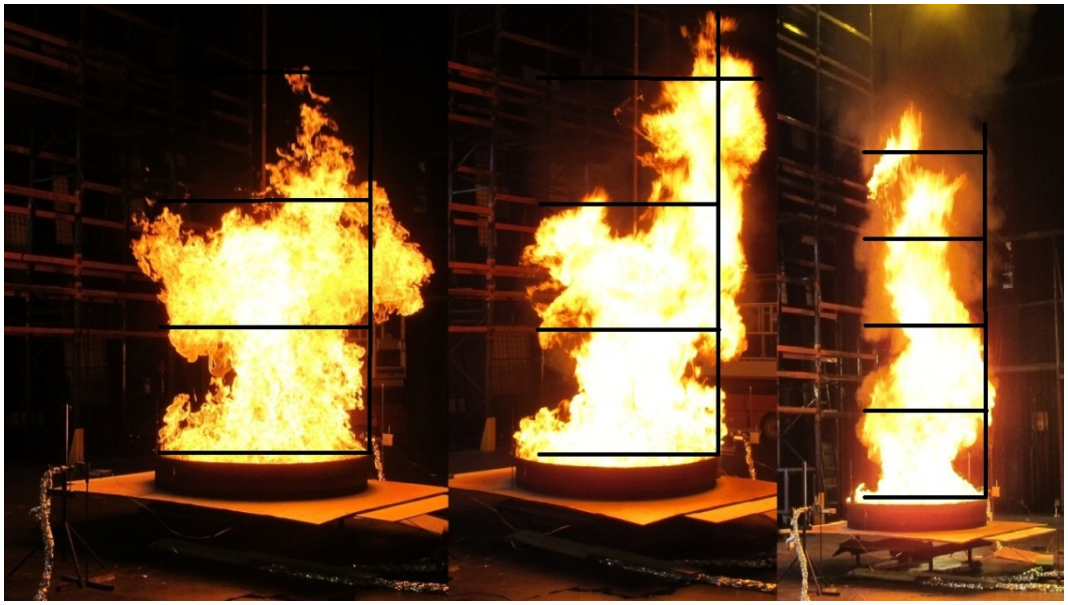

Figure 15 A comparison of the three different fires (E97, E85 and E50, from left to right). Note that E50 (right) is taken from a longer distance due to higher heat exposure.

Two significant visual differences were the smoke production and the flame height. The more gasoline in the fuel mixture, the higher flames were and the more smoke was produced. The E97 fuel had a significantly lower smoke production compared to the others.

A summary of the measurement results from the three fuels is presented in Table 2

Table 2 Summary of the measuring data from the three different fuel mixtures.

Parameter / Fuel	E97	E85	E50
Flame height (m)	2-3	3-4	4-5
Heat flux 1 m from the flame (Vertical measurement) (kW/m^2)	13	17	19
Heat flux 1 m from the flame (Horizontal measurement) (kW/m^2)	6.5	8	10
Heat flux 3 m from the flame (Vertical measurement) (kW/m^2)	4.1	5.6	6.9
Heat flux 3 m from the flame (Horizontal measurement) (kW/m^2)	2	2.5	3
PT temperature 1 m from the flame (Vertical measurement) (°C)	320	380	400
PT temperature 1 m from the flame (Horizontal measurement) (°C)	210	250	290
PT temperature 3 m from the flame (Vertical measurement) (°C)	150	190	220
PT temperature 3 m from the flame (Horizontal measurement) (°C)	75	100	125
Measured heat release rate (kW)[1]	1800	2500	NR
Average burning rate, thermocouple tree (mm/min)	3.0	3.9	4.3
Average burning rate, from mass loss rate (mm/min)	3.0	3.7	4.2
Mass loss rate (kg/min)	4.7	5.8	6.4
Combustion efficiency	0.84	0.88	-
Starting weight (kg)	158.1	153.9	155.8
Radiative fraction[2]	0.5±0.1	0.47±0.1	0.44±0.1

NR = Not recorded due to ventilation flow limitations in the industrial calorimeter system
[1] Total heat release rate
[2] Calculated by the assumption in chapter 4.2.3 about chemical heat of combustion and applying the point source method to the heat flux at 3 m (taking into account both horizontal and vertical heat flux).

4.1.1 Temperature measurements and calculated heat flux

Diagrams showing the measured PT temperatures as a function of time for the three fuels and at 1 m and 3 m are presented in Figure 16. Based on the PT data, the corresponding incident radiant heat flux has been calculated and presented in Figure 17. The results show clearly that the E97 fuel generates the lowest heat flux while the E50 generates the highest. The increasing radiant heat flux is also shown in Figure 18 as a function of the proportion of gasoline in the fuel mixture.

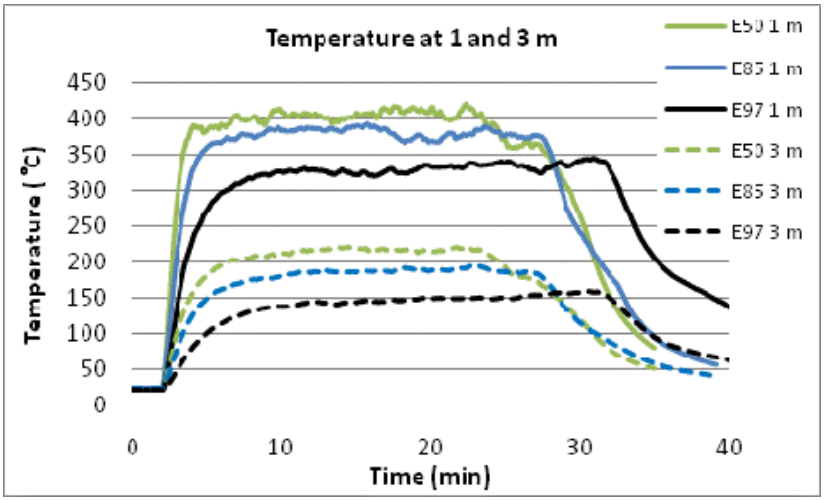

Figure 16 **Comparison of PT temperatures measured at 1 m and 3 m for the three different fuels.**

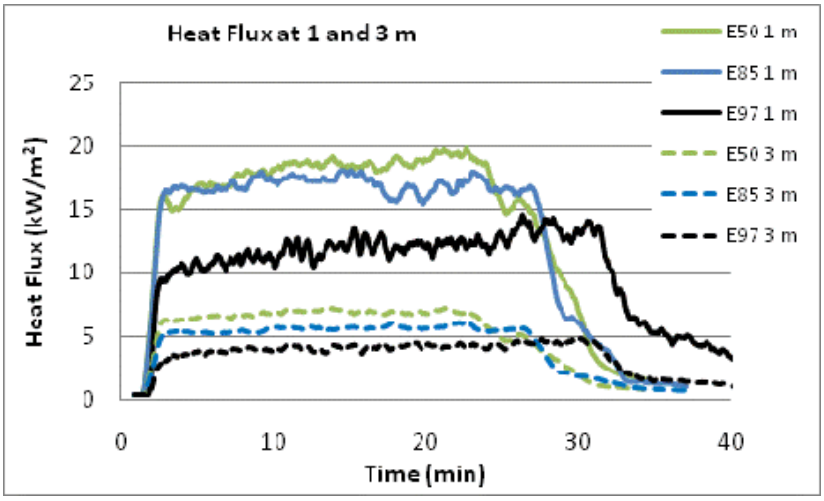

Figure 17 **Comparison of calculated incident radiant heat flux at 1 m and 3 m for the three different fuels.**

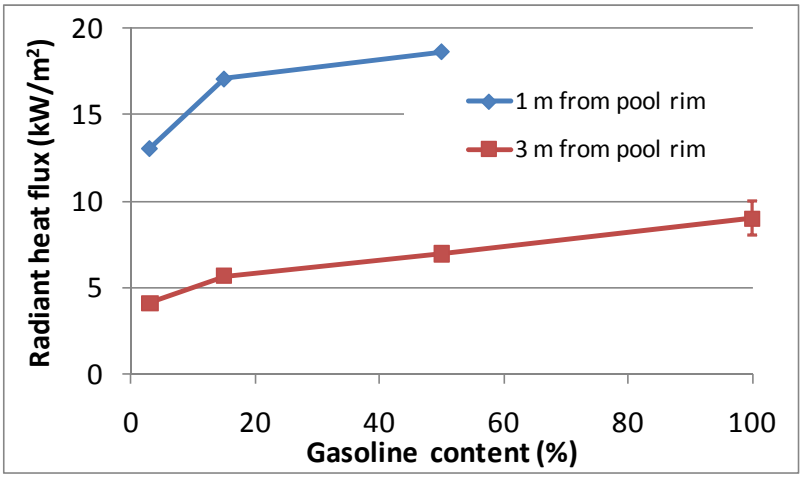

Figure 18 **Average radiant heat flux (between 10 and 20 minutes) as a function of gasoline content in the fuel. The gasoline data is from work by Blom, Ref. [3].**

4.1.2 Comparison between PT and heat flux meter measurements.

In Figure 19, a comparison has been made between the incident heat flux measured with a PT and a heat flux meter at 1 m from the pool rim. The values from the heat flux meter were used as a calibration signal to set the two correction factors for the PT – the loss and storage correction factor (see equation 1). The loss factor gives an additional contribution to the signal proportional to the temperature difference of the PT and ambient gas. The storage correction is only relevant during very transient stages. It corrects for the slower response time of the PT compared to the heat flux meter.

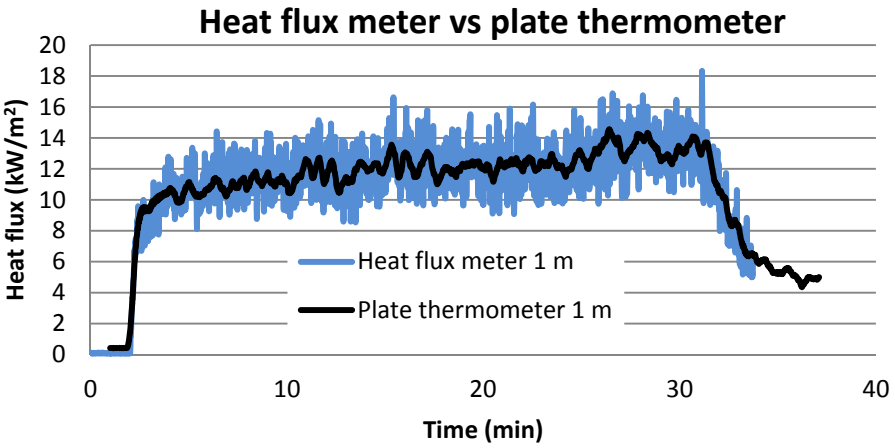

Figure 19 **Comparison of the measured heat flux values using a PT and a heat flux meter at 1 m from the pool rim during the E97 fire test.**

For the purpose of the tests in this project, very fast fluctuations are of minor interest as it is the average heat flux that will cause heating of nearby objects and personnel. As described in chapter 2.1, the PT has the advantage of providing data on the maximum possible temperature of an exposed object, which is of great use during a risk analysis.

Based on these results and the good correlation of data as shown in Figure 19, it was decided to primarily use insulated PT for heat flux measurements during the full scale tests.

4.2 Large scale tests

4.2.1 Flame characteristics

As in the laboratory scale tests, there were some visual differences between the E97 and E85 large scale fire tests. The most significant observation was the increased amount of smoke from the E85 fire. In the E97 test, the entire flame was visible continuously without being obscured by smoke while the top of the flame was partly obscured most of the time in the E85 test. Albeit, the smoke production and the flame obscuration for E85 was still far less than for a petroleum fire, e.g. gasoline or diesel.

Although there were significant fluctuations over the course of the tests, both in the appearance of the flame and the flame height, Figure 20, provides a characteristic "average picture" of the two fuels. The E97 flame is more clear and bright yellow while the E85 includes more orange regions.

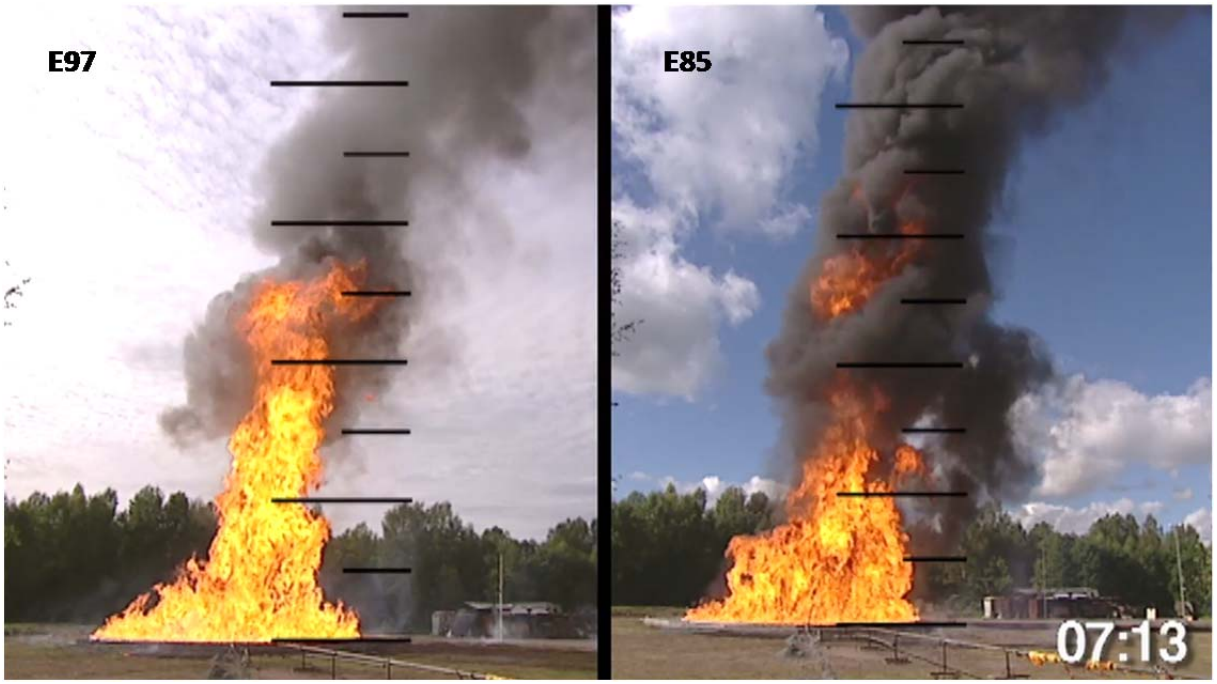

Figure 20 Typical flame characteristics for the two fuels. Both photos are taken 7 minutes and 13 seconds after ignition. The lines represent heights of five meters each.

A frequently used characteristic for flames is the flame height, which is usually defined as the height of the visible yellow or orange in a flame. The visible flame height is here extracted manually from the video recordings. The flame is analysed every 5 seconds from 3 to 11 minutes after ignition, see Figure 21. The average flame height is about 32 m for E85 and 28 m for E97, although there is considerable uncertainty in the measurement. See Appendix 3 for a discussion of uncertainty of estimating flame height.

The flame height was defined as the highest point where flame was visible during one second. For E85 this was often glimpsed through the smoke layer. Thus, the real flame was probably higher for E85 but was not visible due to smoke obscuration.

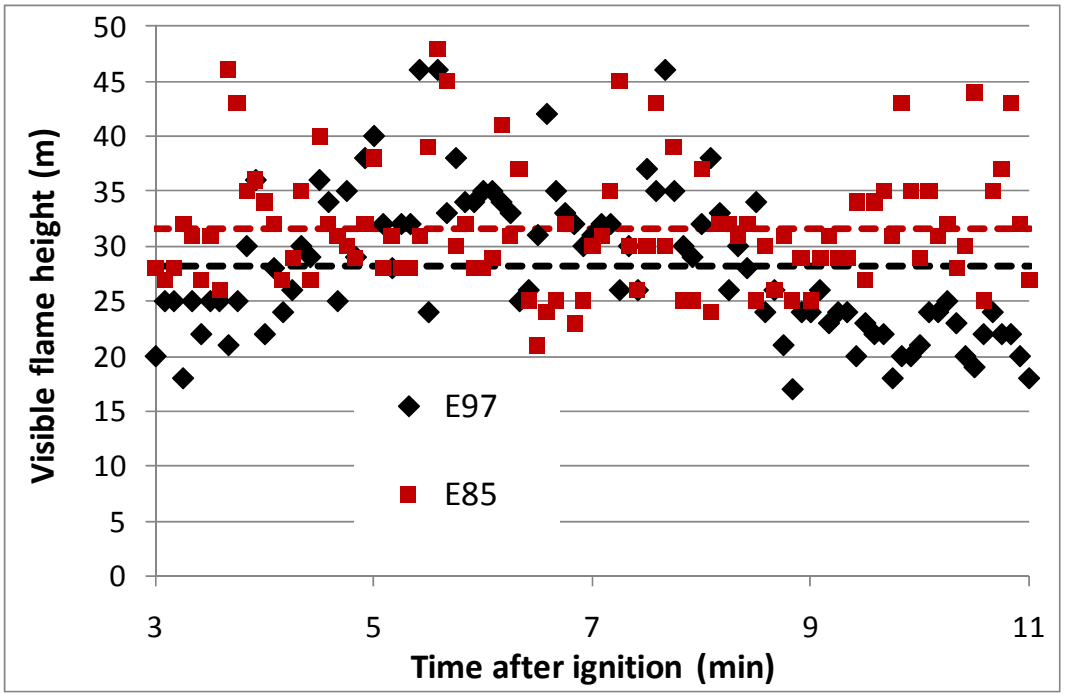

Figure 21 **Visible flame heights, defined by highest position where the flame is visible during one second, points are shown for every five seconds. The dashed lines are the average flame heights over the period 3-11 minutes after ignition.**

A less subjective way of defining flame height is in terms of temperature. Small thermocouples are often used which are affected by both radiation and convection. The temperature of the flame tip is then often defined as a thermocouple temperature of 500 °C [16]. However, for large scale outdoor pool fires convective heat transfer is of minor interest since the thermal transfer to adjacent objects is overwhelmingly through radiation. The radiant heat flux is a strong function of temperature ($\sim T^4$). As an effect of this, temperatures around 500 °C are not very important in this scenario. Therefore, we define the flame height as the highest level where the radiation temperature exceeds 900 °C.

For an objective analysis we use the IR camera results for this analysis. The radiation temperature, T_{rad}, is defined through $\dot{q}''_{IR} = \sigma T_{rad}^4$, where $\dot{q}''_{IR}$ is the radiant heat flux towards a pixel in the IR camera and σ is the Stefan-Boltzmann constant.

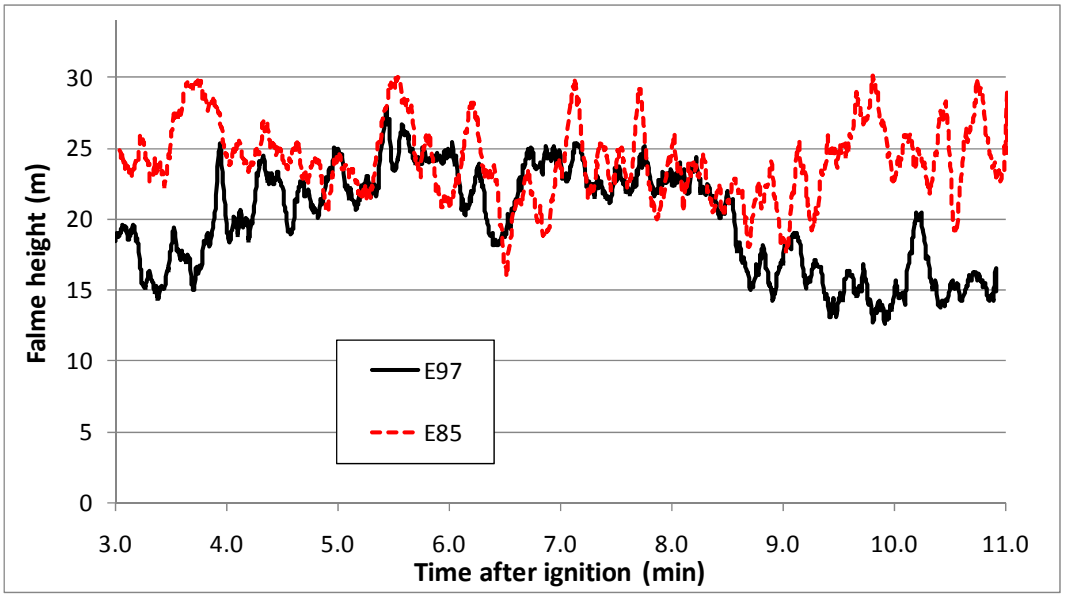

Figure 22 **Flame heights, defined by a radiation temperature above 900 °C for E97 and E85. The data represent five seconds running averages.**

Figure 22 shows fluctuating flame heights for E97 and E85 according to the 900 °C radiation temperature criterion. The E97 flames are between 25 and 27 meters high during the high periods and around 15 m high during low periods. During the period 3-11 minutes after ignition, where steady burning occurs, the E97 flame average is around 20 m, compared to 28 m for visible flames. The flames from E85 are generally higher than from E97, averaging around 24 m for the same period, compared to 32 m for visible flames. The data for E85 should actually be increased by a fraction of a metre since parts of the scatter in the data reaches the upper limit of our instrumentation (above 34 m).

As presented in Figure 21, the height of the visible flame is larger than this IR based definition. Visible flames were sometimes reaching above the video recordings[3] at 40 m. However, the difference between E97 and E85 holds also for the radiation temperature; E85 is a few meters higher based on the available data. However, both in case of radiation and visibility, the upper part of the E85 flame is often obscured by smoke.

4.2.2 Burning rates

The burning rates were measured with the thermocouple tree placed in the centre of the pool. The time estimated for each fuel height is the time of the last recorded temperature below 100 ºC of that specific thermocouple. The E85 burns a little faster, at 5.6 mm/min, compared to E97 with 5.3 mm/min as seen in Figure 23. The difference between E97 and E85 (E85 burns 5.5 % faster) can at least be partly explained by the different energies needed to vaporise the fuel. Given a heat of vaporisation [17] of 837 kJ/kg for ethanol and 349 kJ/kg for gasoline and a specific heat of 2.01 and 2.39 kJ/kgK for ethanol [18] and gasoline [19], respectively, we can estimate the energy required for heating the fuels from 20 °C to boiling and thereafter evaporating it. This energy corresponds to 941 kJ/kg for E97 and 880 kJ/kg for E85; this energy is 6.9 % higher for E97 than for E85.

[3] The maximum height coverage changed during the video recording due to zoom-out actions. The lowest coverage is 40 m. However, the photos in fig. 20 show a higher coverage.

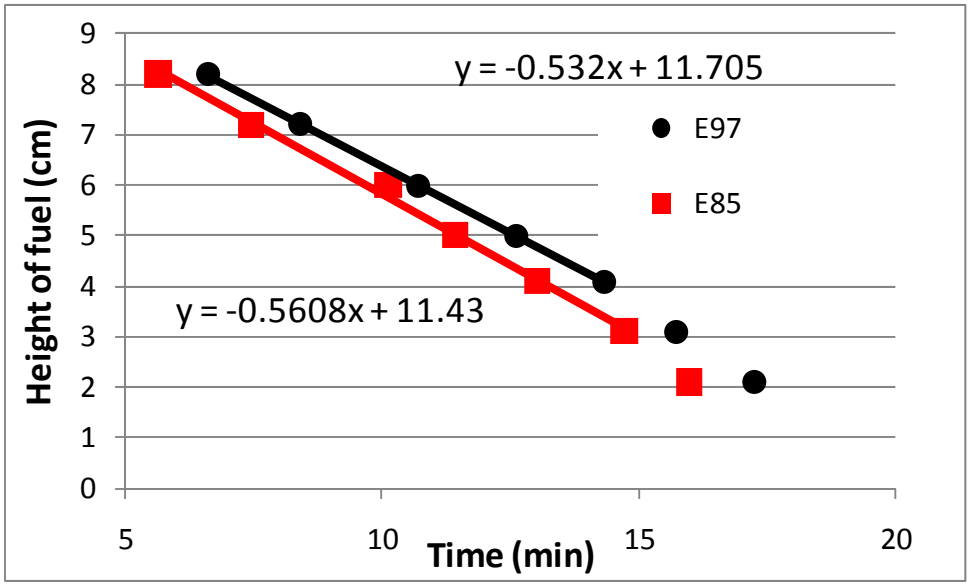

Figure 23 **Depth of the burning fuel as a function of time based on the thermocouple tree measurements. The solid line represents the data used for the burning rate calculation.**

4.2.3 Heat release rates

According to the SFPE Handbook [6] for lower heating values (total heat of combustion per unit mass of fuel minus heat of evaporation), the heat of combustion, ΔH_c, for ethanol and gasoline is 26.8 and 43.7 MJ/kg, respectively. Assuming that the tested fuel mixtures behave as weighted averages of the two constituents, ΔH_c is 27.3 and 29.3 MJ/kg for E97 and E85, respectively. Using the burning rates presented in Figure 23, the total heat release rates are 488 and 548 MW. These values represent complete combustion and do not take into account incomplete combustion, which is normally assumed to increase with increasing size of the fuel pool.

4.2.4 Temperature measurements with PT

The raw PT data is the temperature of the exposed steel plate, which is due to exposure to radiation and convection. The PT located at the rim of the fire test pool were exposed to direct flames which means the measured temperature is achieved by severe radiation and convection from the hot flame. When there is no actual flame impingement on the PT the convective part of the total exposure becomes negative, i.e. it cools the steel surface.

Due to the design of the PT, the recorded temperatures can be interpreted as the maximum surface temperature that any object at the same distance, facing the same direction, can obtain. In most cases the temperature will be lower than this maximum due to heat losses through conduction into the object, e.g. a tank wall will be significant cooled by the product below the product level while the tank wall above the product level only is cooled by the fuel vapours inside the tank and thereby could be closer to the PT measurements.

4.2.4.1 Temperature results from E97 test

During the E97 test, the wind was predominantly blowing from the south with a velocity of 2-4 m/s. This resulted in an increased exposure in the downwind (north) direction which can be seen from the temperature measurements. Steady state temperatures were reached after about one minute at the rim of the pool where flames were impinging the surfaces of the PT. Further away, the temperatures stabilised after 2-3 minutes, see Figure 24.

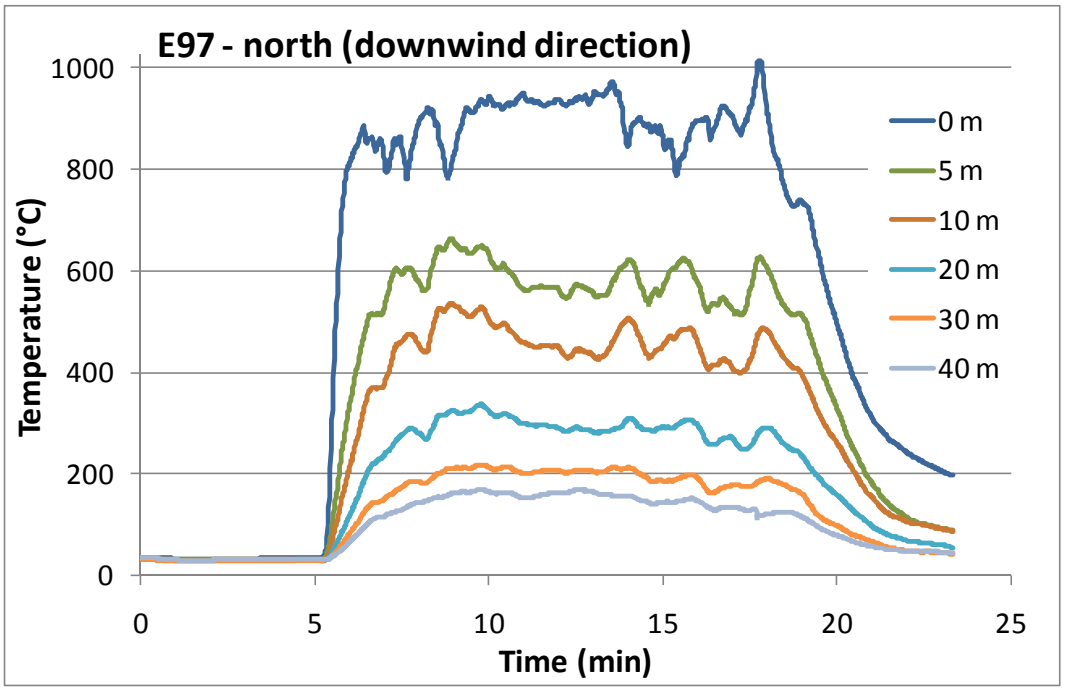

Figure 24 **Temperatures of the PT in vertical positions (facing the fire) along the north (predominantly downwind) direction during the E97 test. The different curves represent different distances from the rim of the pool.**

In Figure 25, the average temperatures during the steady state burning are shown as a function of distance from the pool rim for the different directions. The PT in the downwind (north) direction reaches up to 150 °C higher temperatures compared to the other directions. However, as the distance from the rim of the pool increases, the differences between the different directions decrease. This has mainly two causes: (i) the difference in view factor decreases, which results in less difference in incident radiation and (ii) the hot gases from the fire do not reach the PT and thus the differences in convective cooling decrease. The temperatures of the PT reached a maximum of around 200 °C even for a distance of 30 m. The decline at further distances is slow with temperatures above 150 °C also at 40 m distance.

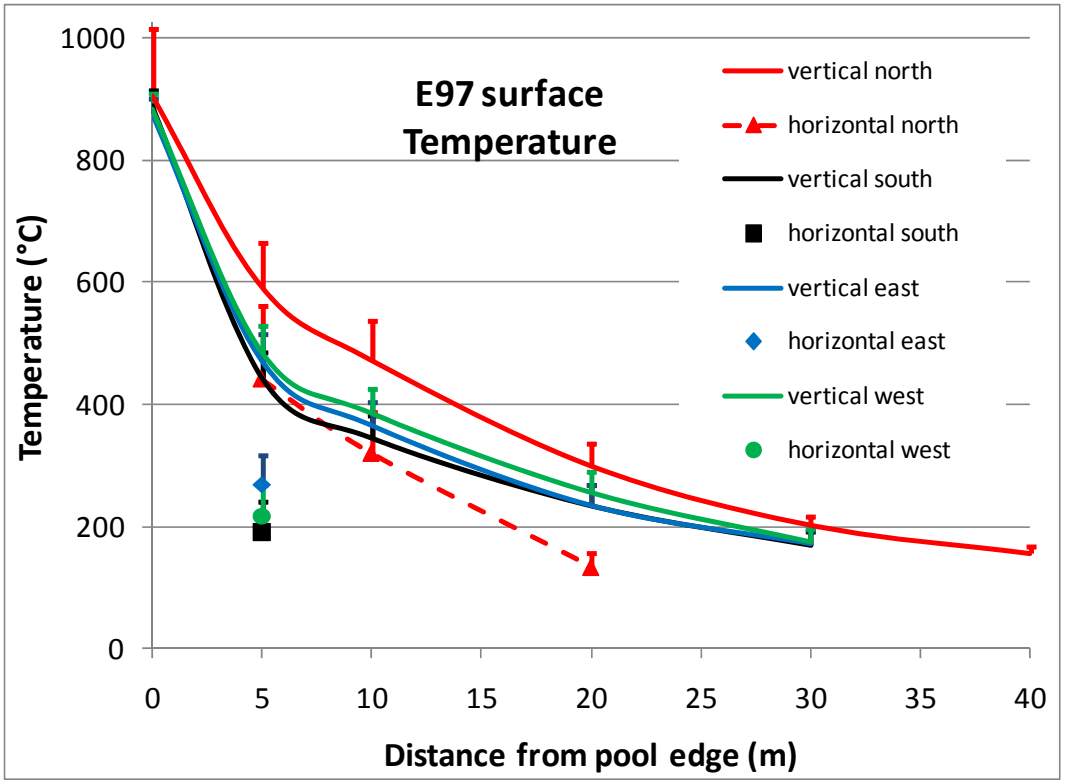

Figure 25 **Average temperatures of the PT located in plane with the pool rim. The average temperature is calculated during the steady state burning taken between 8 min and 16 min into the test (3-11 min from ignition). The vertical bars in the curves indicate the peak values experienced during this time period. The downwind direction was predominantly the same as the north direction.**

The horizontally placed PT (facing the sky) experienced a much lower temperature compared to the vertical ones. Nevertheless, five meters from the pool rim these temperatures average at 440 °C in the downwind direction and between 200°C – 300 °C in the other directions.

A comparison between the PT situated in the plane of the pool and the elevated PT (6.1 m above ground) is shown in Figure 26. For the vertical surfaces, the elevated PT reach a higher temperature compared to the one at pool level while the elevated, horizontally located PT obtained a lower temperature compared to pool level. These are reasonable results given the geometry of the flame. The elevated vertical PT will experience more radiation due to an increased view factor between flame and PT compared to pool level. However the elevated horizontal PT will experience the contrary since it will not “see” the first 5.5 m of the flame.

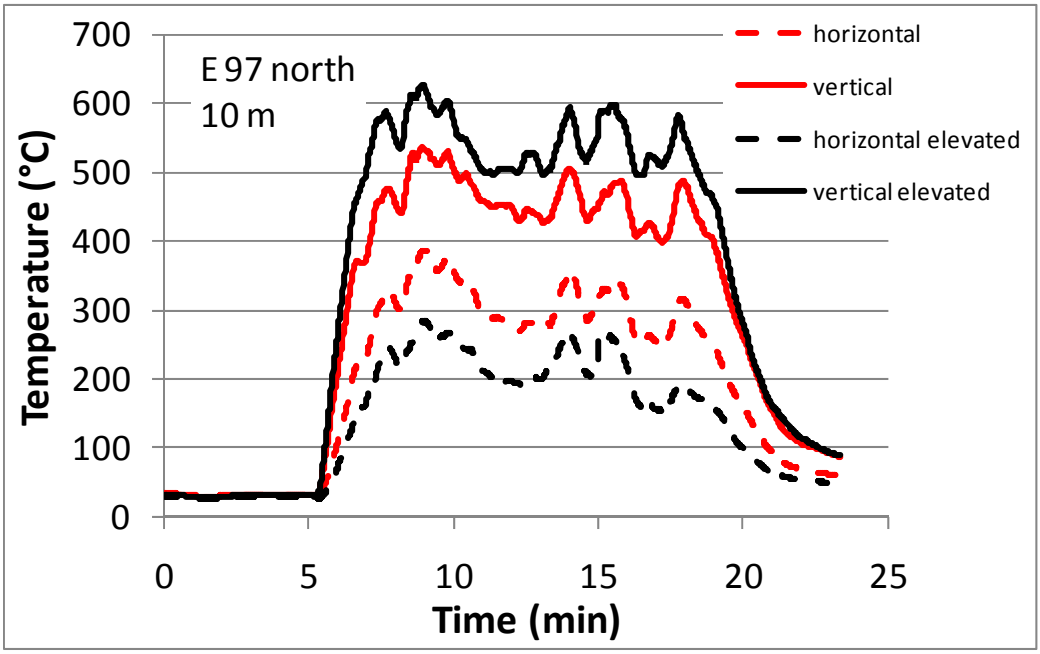

Figure 26 **Comparison of temperatures between PT at pool level and elevated PT, all at a radial distance of 10 m from the pool rim in the downwind (north) direction for the E97 test. The solid and dashed lines represent vertically and horizontally located PT, respectively.**

4.2.4.2 Temperature results from E85 test

The weather conditions during the E85 test were very similar to the E97 test, and so increased temperatures in the north (downwind) direction were also obtained. These are shown in Figure 27.

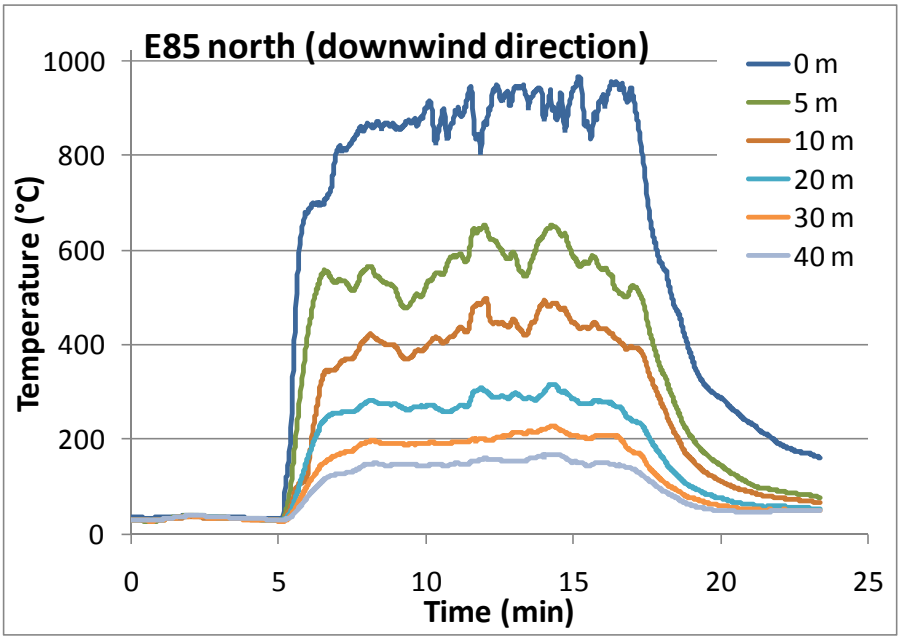

Figure 27 **Temperatures of the plate thermometers in vertical positions (facing the fire) along the north (predominantly downwind) direction during the E85 test. The different curves represent different distances from the rim of the pool.**

The differences between horizontally and vertically located PT were almost the same as for the E97 test; this is shown in the appendix where all results are available. The largest difference is the vertical PT at 10 m radial distance from the pool rim and elevated 5.5 m, see Figure 28. This is about 100 °C colder compared to the results from E97 and thus does not significantly exceed the values from the same radial distance at pool level. This is possibly a consequence of the increased smoke production in E85, which obscures the radiation at larger heights.

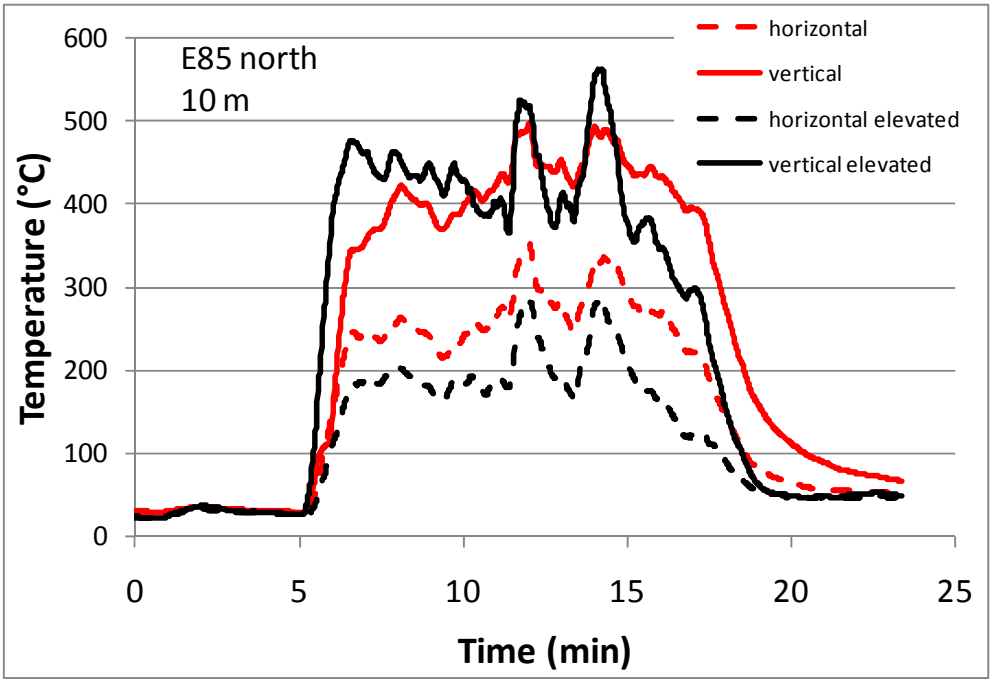

Figure 28 **Comparison of temperatures between PT at pool level and those elevated 5.5 m, all at a radial distance of 10 m from the rim of the pool in north (downwind) direction for the E85 test. The solid and dashed lines represent vertically and horizontally located PT, respectively.**

4.2.5 Overall comparison between E97 and E85

Despite the differences in burning rate and smoke production, the overall temperatures of the PT are very similar between the two tests. Even though the scatter is different, the average values as well as the magnitude of the extreme values at each distance are very similar. By averaging all PT over the steady state burning period (3 – 11 minutes from ignition), the scatter and the difference due to the shorter duration of the E85 fire is removed. In addition, averaging each distance over all directions removes any differences in wind direction. These averaged temperatures are astonishingly similar between E97 and E85 as seen in Figure 29. Only a few degrees difference for average temperatures at each distance is noticeable between the two fuels. The only difference is a slightly larger spread in the scatter for the E97 test. These similar results are inconsistent with the differences noticed in the laboratory scale tests. A conclusion from this is that 254 m^2 pool fires of E85 or E97 will have the same thermal impact on the surrounding if the weather conditions are the same.

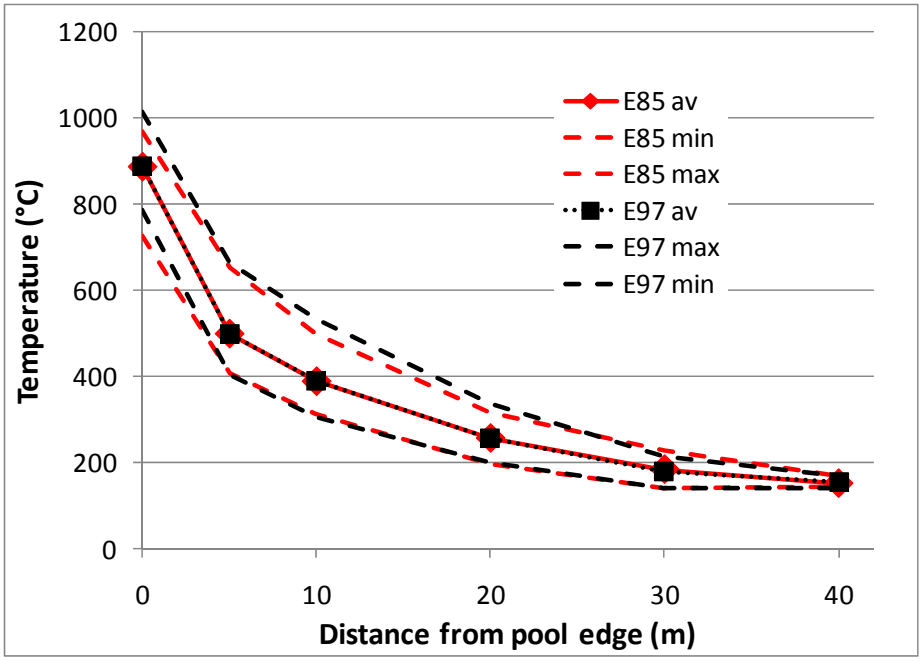

Figure 29 **Temperatures of vertically placed PT averaged both over time during the steady-state burning period (3-11 min after ignition) and over all directions. The dashed lines show the maximum and minimum values of any PT at that distance at any time or direction.**

4.2.6 Calculated radiant heat flux for E97 and E85

Based on the temperature measurements, the heat flux has been calculated for all measuring positions. Recall that these values are for heat fluxes towards a vertically oriented surface. As with temperatures, the radiation levels of the two different experiments are very similar. The radiation from E97 is higher with respect to the maximum values recorded both upwind and downwind. However, the difference is mostly well within 10 %. The average values of radiant heat flux during steady state burning are the same for both fuels. Figure 30**Fel! Hittar inte referenskälla.** shows the Radiant heat flux in downwind and sidewind direction as a function of distance.

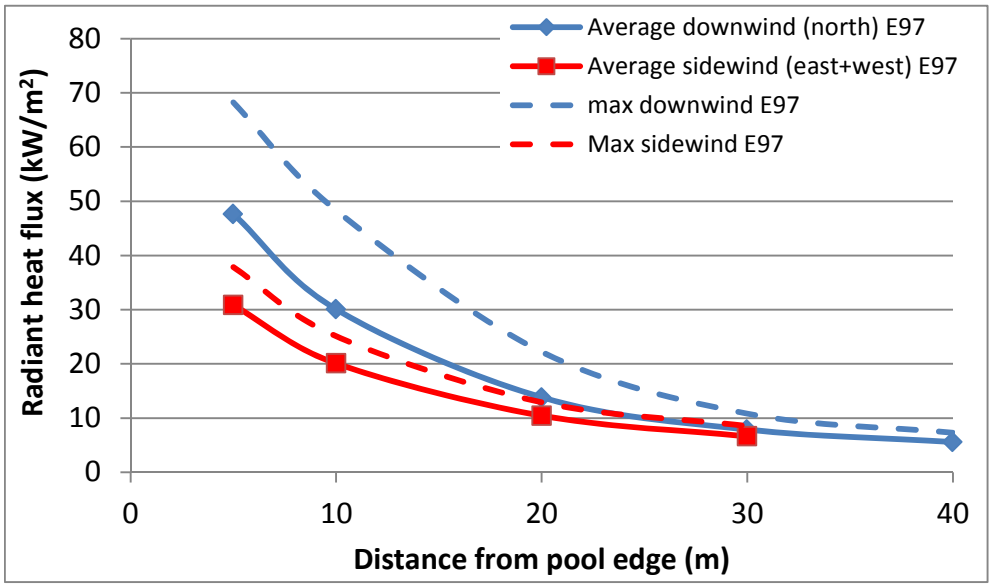

Figure 30 **Average values of radiant heat flux (3-11 minutes from ignition) towards a vertical surface for different distances from pool rim. Results are for E97 in downwind and sidewind directions. The dashed lines represent peak values during this period.**

The radiant heat flux reported here is to a vertical surface. A surface oriented slightly more towards the center of the flame would receive more heat flux than a strictly vertical one. How much larger this heat flux to an "optimally oriented surface" is difficult to estimate without a full description of flame geometry and temperature distribution. A quick and popular method is the point source method which uses the radiant heat flux in vertical and horizontal direction and to calculate the radiant heat flux towards a surface which is oriented to receive optimum (worst case) radiation by:

$$\dot{q}''_{opt} = \sqrt{\dot{q}''^2_H + \dot{q}''^2_V} \tag{3}$$

where *H* and *V* represent horizontal and vertical orientation, respectively. However, for a distributed flame this method overestimates this heat flux if the object receiving the radiation is close to the flame.

Using the heat fluxes shown above we can use the calculated chemical heat of combustion to estimate the radiative fraction of the fire. The radiative fraction is defined in equation 4 as the fraction of the chemical heat release rate which is radiated away from the flames:

$$\chi_{rad} = \frac{\dot{Q}_{rad}}{\dot{Q}_{chem}} \tag{4}$$

The other components of the chemical heat release are the convective heating of the gases and the effects of incomplete combustion. To calculate the radiated heat release we apply the point source method to the most distant measuring points. The point source method assumes that radiation is emitted isotropically, that is, with equal intensity in all

directions. This assumption becomes better as the distance from the fire increases. Thus, the radiant heat flux decreases with the square of the distance to source[4].

$$\dot{q}''_{rad} = \frac{\dot{Q}_{rad}}{4\pi r^2} \quad (5)$$

With equation 5 above we calculate the radiative fraction to be χ_{rad} = 33 (±2) % for E97 and 30 (±2) % for E85.

4.2.7 Accuracy of the radiative heat flux measurements

The calculation of incident radiant heat to the PT is based on the algorithm described in chapter 2.1. In this calculation we use simplifications and assumptions that will naturally have an impact on the precision of the results. A discussion concerning the accuracy of calculating the incident heat flux from PT measurements is found in Ref [20].

[4] This fraction is calculated using a corrected distance to the centre by 2 m due to the inclination of the flame. It is also assumed that the height of the point source is 8 metres. However, varying this height between 4 and 15 m only changes the fraction by 1 %.

5 Discussion and conclusions

5.1 Laboratory scale versus large scale

For the 2.0 m^2 pool fire there was a clear trend in increased radiation from the flames as the gasoline content of the fuel increased, from 4.5 kW/m^2 for E97 to 5.5 kW/m^2 for E85 to 7.0 kW/m^2 for E50 at a distance of 3 m from the pool rim. A re-calculation of previous measurements [3] using an pool area of 1.73 m^2 applied to the 2.0 m^2 pool area used in this project, show that commercial gasoline would give a corresponding heat flux of about 9 kW/m^2.

However, this behaviour is not found in the experiments with larger pool areas. The E97 and E85 fuel emitted the same radiant heat flux towards its surrounding. Thus, increasing the hydrocarbon content of the fuel will not increase the radiant heat flux (as we will see below, it actually decreases for pure gasoline). There are several reasons for this, the main ones are listed below:

- The combustion becomes less complete for fuels with longer hydrocarbon chains. As the pool size is increased the central part of the pool fire becomes more oxygen deprived, leading to incomplete combustion and more smoke production. This is particularly evident for longer-chain hydrocarbon mixes such as gasoline, which are more prone to produce smoke compared to short-chain alcohols such as ethanol [2, 4].
- A substantial portion of flames from large pools of hydrocarbon fuels can be obscured by smoke that covers the outer parts of the flame. The smoke absorbs radiation from the hot flames. A larger portion of gasoline increases the smoke production, which produces a larger effect for E85 compared to E97. In these experiments a higher smoke production from E85 was clearly apparent compared to E97 [5]. Thus, the increased smoke production balances the higher heating value of combustion of E85 compared to E97.
- For a small flame, the flame emissivity of a short-chain alcohol could be substantially reduced compared to gasoline while the emissivity is close to 1.0 for both fuels in large scale (flame emissivity is discussed in Appendix 8, Basic theory).

The pool size dependence of burning rate, and radiant fraction have been studied for many hydrocarbon fuels. The burning rate increases with pool size for small pool areas before it saturates to a constant value. This means that the evaporation rate, as mass per unit time, increases proportionally to pool area for large pools. Despite this, the radiation experienced at a distance does not follow the same increase. Thus, the fraction of heat being radiated from the flame decreases rapidly with increasing pool size.

Figure 31 shows values of mass loss rate from pool fires of gasoline and the mass loss rates from our experiments for E97. They do not differ significantly between each other.

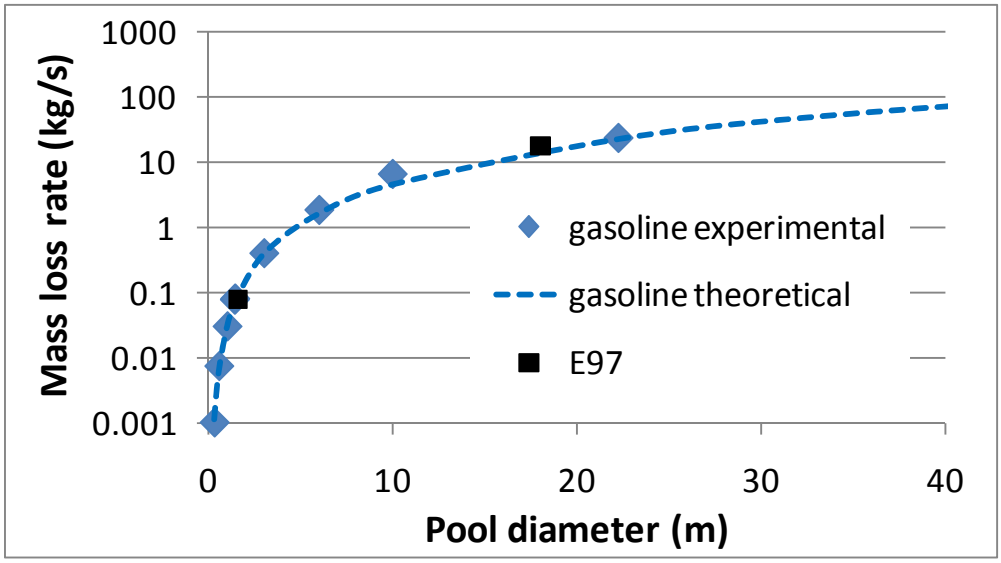

Figure 31 **Mass loss rates for gasoline from literature (redrawn from Ref. [2]). Included is also the mass loss rate from our experiments.**

Figure 32 however, shows the radiative fraction for gasoline and other hydrocarbon fuels. The experimental data is very consistent and follows the same behaviour. The radiant fraction is constant for small pool sizes (around 30 to 50 %) but decreases rapidly above pool diameters of ~2 m. The decrease is dramatic and for pool diameters of 20 m the radiative fraction is about 5-10 %.

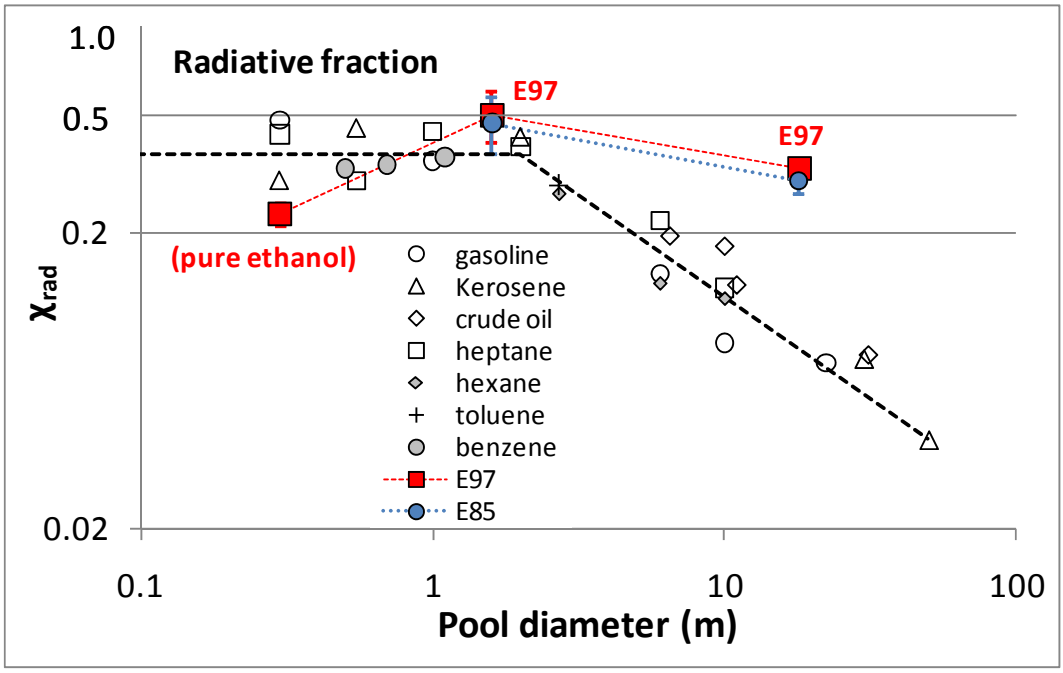

Figure 32 **Radiative fractions for hydrocarbon fuels (open and grey symbols) for different pool sizes (redrawn from Ref. [2]. Included are the test results of this study for E97 and a small pool fire of pure ethanol [21]. Both axes are on a logarithmic (base 10) scale.**

For E97 the situation is not the same. The radiative fraction does not decrease as dramatically as for hydrocarbon fuels. This is the most important fact which makes

conclusions about hydrocarbon fuels vs. alcohol for large scale fires drawn from laboratory scale experiments invalid.

5.2 Comparison to gasoline

One main goal with the test series was to study the difference in heat flux between various ethanol fuels and gasoline during large scale conditions. Since no test was made with gasoline in this project, results from various calculations have been used to compare gasoline with the ethanol test data. As a basis for this comparisons, the software Phast (version 6.7) from Det Norske Veritas, and the Shell software FRED (version 6.0.0.16), were used for calculation of incident heat flux for gasoline using conditions similar to the large scale tests.

Shell software FRED (Fire, Release, Explosion, Dispersion) is a consequence modeling software. One of its many components is pool fires, which has been used in this case. FRED has default values for calculations with gasoline.

Phast (Process hazard analysis software tool) is also consequence modeling software. Phast does not have gasoline as a default product in the system. The procedure is to use a similar fuel or assemble a fuel. In this case, since gasoline is a mixture of many hydrocarbon fractions, the best choice was to choose a similar fuel. This version of Phast does not consider the change in properties when mixing fuels.

To achieve the best possible similarity to gasoline, two different types of available fuels were tested. The fuels that are usually used to resemble gasoline are either N-Hexane or N-Octane. To study the difference between these two, the incident heat flux was compared and is shown in Figure 33.

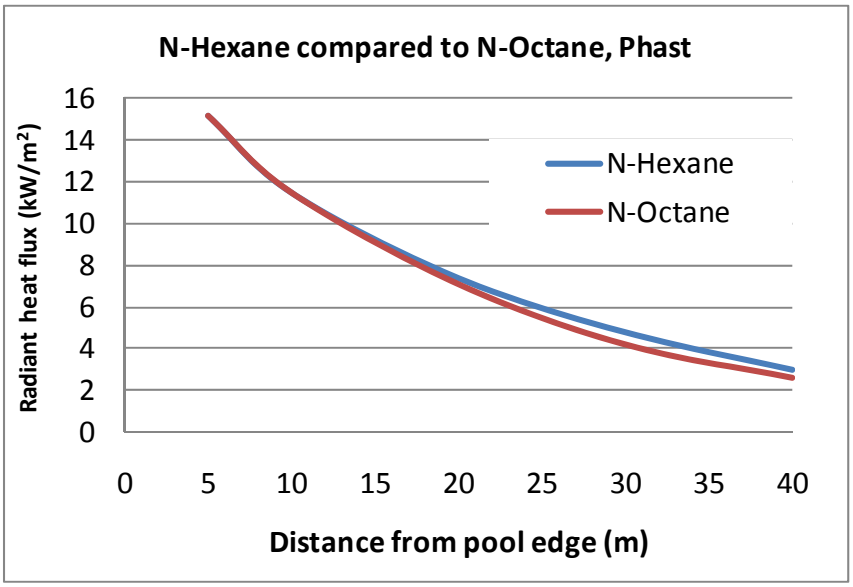

Figure 33 **Comparison of incident heat flux when using N-Hexane and N-Octane as fuels in Phast. The input values (weather, pool size etc.) are the same as in the ethanol tests.**

As shown in Figure 33, there is only a small difference in incident heat flux between the two and so, for conservative reasons, N-Hexane has been used for further calculations. A

summary of the input data used for the Phast and FRED calculations are presented in Table 3 and Table 4, respectively.

Table 3 Parameters for N-Hexane used in the Phast calculations.

Parameter	Value	Unit
Wind speed	2	m/s
Relative humidity	50	%
Burning rate	0.097	kg/m^2s
Flame emissive power	33.83	kW/m^2
Normal boiling point	68.73	°C
Radiative fraction	0.07	
Molecular weight	86.18	g/mol
Lower flammable limit	10500	ppm
Upper flammable limit	76800	ppm
Heat of combustion	$3.855 \cdot 10^6$	kJ/kmol
Flash Point	-21.65	°C
Flame	Smoky	
Max Surface Emissive Power	140	kW/m^2
Vapor pressure, Density and Heat capacity are calculated via Dippr equations.		

Table 4 Parameters for gasoline in the FRED calculations

Parameter	Value	Unit
Wind speed	2	m/s
Relative humidity	50	%
Mass burning rate	0.055	kg/m^2s
Average surface emissive power	40	kW/m^2
Burning rate size coefficient	2	/m

A comparison of the measured heat flux data for E97 and the calculated heat flux for gasoline is shown in Figure 34 to Figure 36. The three figures present the results for all directions, downwind, perpendicular to the wind, and upwind. Experimental data has also been included from previous large scale tests [1, 2]. In the two gasoline tests conducted in 1990 [1], the measurements were made in a mostly perpendicular orientation to the wind but some downwind components were also present as described below. The results are included in Figure 35. It should be noted that the pool area in those tests was slightly less (197 m^2) and the pool was a combination of a circular (Ø = 13.4 m, equal to 141 m^2) and a rectangular pool (7.6 x 7.3 m, equal to 56 m^2) forming a rectangular area with a total length of 21 m in the direction pointing towards the installed heat flux meters. Not only are the pool sizes different in the comparisons. The tests 197 m^2 tests were subject to gusty wind conditions, both in wind velocity and wind direction. Certain intervals of the tests were measured partly in downwind direction. Other test results (Ref. [2]) are also shown. These are for both larger and smaller pool sizes (79 as well as 390 m^2).

Although there is a slight difference between the FRED and Phast data, both of them predict significantly lower heat flux values for gasoline compared to the measured values for E97. This is also verified by the experimental data.

As previously mentioned, there were only minor differences between E85 and E97 in the large scale tests and the comparion below is therefore also valid for E85 in this scale.

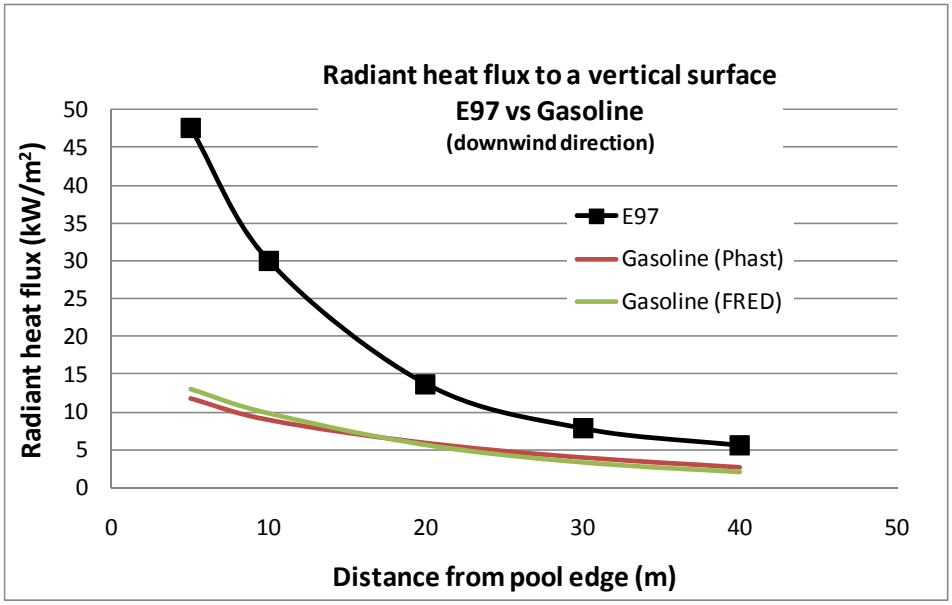

Figure 34 **The difference in heat flux between E97 and gasoline at different distances from the pool rim in the downwind direction.**

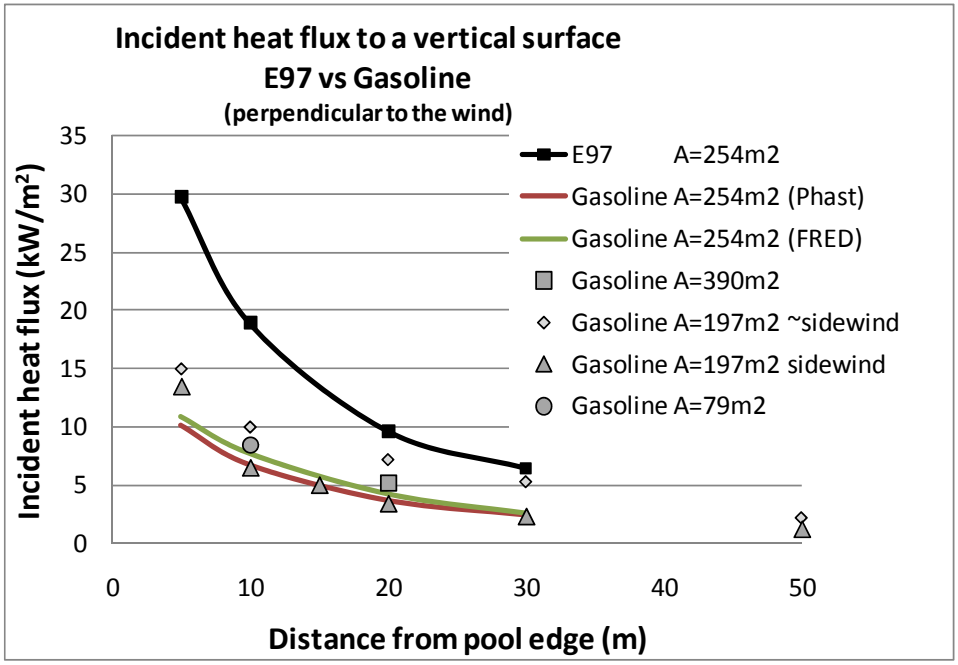

Figure 35 **The difference in heat flux between E97 and gasoline at different distances from the pool rim perpendicular to the wind direction. The gasoline data are both from Phast and Fred as well as available experimental data from different pool sizes (197 m^2 from Ref [1] and 390 as well as 79 m^2 from Ref. [2]). Note that the two experiments on gasoline for 197 m^2 were conducted in gusty wind conditions and the heat flux meters were slightly in downwind direction.**

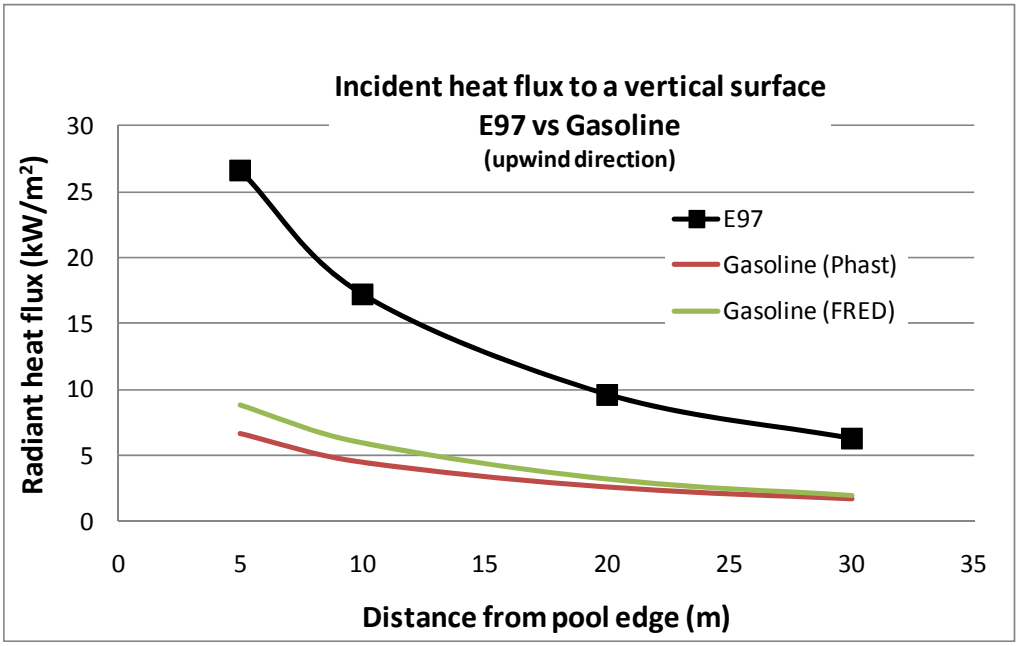

Figure 36 **The difference in heat flux between E97 and gasoline at different distances from the pool rim in the upwind direction.**

In order to better understand the consequences of the different heat flux levels for gasoline and E97, a comparison has been made in Table 5 to show how this heat flux will result in heating of an exposed steel surface. In the E97 tests, these temperatures directly correspond to the temperature measurements with the PT. For gasoline, the results from the FRED simulation have been used, partly because such corresponding steel temperatures can be obtained directly from the calculations, and partly because the FRED results are slightly more conservative.

Table 5 **Calculated temperatures of a vertical steel surface at various distances during a gasoline fire using the FRED software compared to the PT measurements during the E97 fire.**

Position	Calculated temperatures for vertical steel, gasoline (FRED) (°C)	Average measured temperature for E97 with PT (°C)
Sidewind 5 m	268	471
Sidewind 10 m	211	366
Sidewind 20 m	137	235
Sidewind 30 m	94	173
Downwind 5 m	303	592
Downwind 10 m	253	473
Downwind 20 m	172	300
Downwind 30 m	117	203
Downwind 40 m	83	157
Upwind 5 m	234	443
Upwind 10 m	178	345
Upwind 20 m	112	234

In order to interpret the consequences of various heat flux levels, it is also interesting to relate the results to some reported effects on humans and the risk for ignition; in Table 6 some data is compiled from Refs. [6, 22].

Table 6 Observed effects of different heat fluxes.

Heat flux (kW/m^2)	Observed effect
1	Maximum level for unprotected skin
2.9	Pain after 30 seconds of skin exposure
4-5	Workable conditions for firefighters
6.4	Pain after 8 seconds of skin exposure
8	Maximum limit for short work periods for firefighters
12.5	Pyrolysis of wooden material, ignition with a small flame
29	Wood ignites without the presence of a pilot flame
52	Wooden board ignites within 5 seconds without pilot flame

5.3 Conclusions

The free-burning tests conducted within this project clearly show that there is a significant difference in burning behavior of ethanol fuels in small and large scale, and that laboratory scale tests cannot be used to predict large scale burning behavior. In particular this is relevant for predicting the heat exposure towards nearby objects due to incident heat flux generated by the fire.

The large scale results show that the heat exposure towards the nearby surroundings (within 5 m) is on the order of 3 times higher for the E97 and E85 fuel compared to calculated and experimental data for gasoline. The difference decreases with distance from the pool rim but is still in the order of a factor 2 higher at 30-40 m.

In these tests, the heat flux generated by the E97 and E85 fires was almost the same. The radiative fraction as a function of fire area will probably have a larger influence on E85 compared to E97 due to the higher content of gasoline, so it is likely that a larger E97 fire would generate a higher heat flux compared to a similar E85 fire and the difference between the two would increase with increasing fire area.

The differences between gasoline and ethanol are influenced by the size of the fire and are only relevant for the fire area (about 250 m^2) used in these tests. If the fire area increases, the difference between gasoline and E97 would probably also increase because the radiative fraction from the E97 fire appears to be only slightly influenced by the fire area while the radiative fraction for gasoline is significantly reduced as the fire area increases.

In order to estimate the heat exposure from fires under various conditions, and thereby be able to judge the consequences in a real industrial environment, software like Phast and FRED are needed. However, in order to obtain reliable results, it is important that differences in fire behavior between fuel types is considered, such as the differences between ethanol and gasoline observed in these tests.

6 References

[1] Persson, H., ”Fundamental equipment for foam firefighting – Experimental results and recommendations as a basis for design and performance”, SP-Rapport 1990:36 (in Swedish).

[2] Koseki, H., “Combustion Properties of Large Liquid Pool Fires”, Fire Technology vol. 25, p. 241 (1989).

[3] Blom, J., ”Jämförelse av E85 respektive bensins brandegenskaper”, SP Arbetsrapport, P603373, 2006.

[4] Steinhaus, T., Welch, S., Carvel, R. and Torero, J., “Large-scale pool fires”, Thermal Science 11 (2007) 101-118.

[5] McGrattan, K. B., Baum, and H. R., Hamins, A., “Thermal Radiation from Large Pool Fires”, NISTIR-6546, NIST, Gaithersburg, Md., USA, 2000.

[6] SFPE Handbook of Fire Protection Engineering, 4th edition, 2008.

[7] Persson, H., Lönnermark, A., ”Tank Fires-Review of fire incidents 1951-2003”, SP Report 2004:14.

[8] Personal communication with Chief Superintendent Hans Bootsma, Port Kembla ethanol tank fire, 2004.

[9] Personal communication with Captain Mathieu Perrin, Industrial Fire Prevention Service, France.

[10] Personal communication with George Cajaty Barbosa Braga, University of Brasilia; http://g1.globo.com/sp/bauru-marilia/noticia/2013/01/incendio-em-tanque-de-alcool-em-usina-em-ourinhos-continua-apos-24h.html; http://g1.globo.com/sp/bauru-marilia/tem-noticias-2edicao/videos/t/edicoes/v/incendio-em-tanque-de-alcool-em-usina-de-ourinhos-e-controlado-depois-de-30-horas/2331385/

[11] Wickström, U., The plate thermometer - a simple instrument for reaching harmonized resistance tests, Fire Technol. 30 (1994) 195-208.

[12] Ingason, H. and Wickström, U., ”Measuring incident radiant heat flux using the plate thermometer” Fire Safety Journal (2007) vol. 42, pp. 161–166.

[13] Holman, J.P., ”Heat Transfer 6th ed.” McGrw-Hill, New York, 1986.

[14] Häggkvist, A., Sjöström, J. and Wickström, U., ”Using plate thermometer measurements to calculate incident heat radiation”, J. Fire Sci. (2013) vol. 31, p. 166

[15] Medtherm models 64-10SB-18, 64-20SB-18 for laboratory scale tests, and models 64-5-18, 64-2-18 for large scale tests.

[16] Heskestad, G., “Flame Heights of Fuel Arrays with Combustion in Depth”, pp. 427-438 in Fire Safety Science-Proc. 5th Int. Symp., Int. Assn. for Fire Safety Science (1997).

[17] “Alcohols: A Technical Assessment of Their Application as Motor Fuels,” API Publication No. 4261, July 1976.

[18] “Data Compilation Tables of Properties of Pure Compounds,” Design Institute for Physical Property Data, American Institute of Chemical Engineers, New York, 1984.

[19] “Status of Alcohol Fuels Utilization Technology for Highway Transportation: A 1981 Perspective,” Vol. 1, Spark-Ignition Engine, May 1982, DOE/CE-56051-7.

[20] Sjöström, J. and Wickström, U., “Different types of plate thermometers for measuring incident radiant heat flux and adiabatic surface temperature”, Proceeding of Interflam ‘13, London, 2013.

[21] Fang, J. et al, “Influence of low air pressure on combustion characteristics and flame pulsation frequency of pool fires”, Fuel vol. 90, p. 2760 (2011).

[22] Ondrus, J., “Brandförlopp”, LTH, Lund 1989 (Swedish).

Appendix 1 - Accuracy of measurements

Accuracy of thermocouple temperatures.

The thermocouples used in these experiments were shielded type K thermocouples. These are all controlled for temperature according to IEC 60584. The maximum allowed error for these thermocouples is shown in Figure A 1.

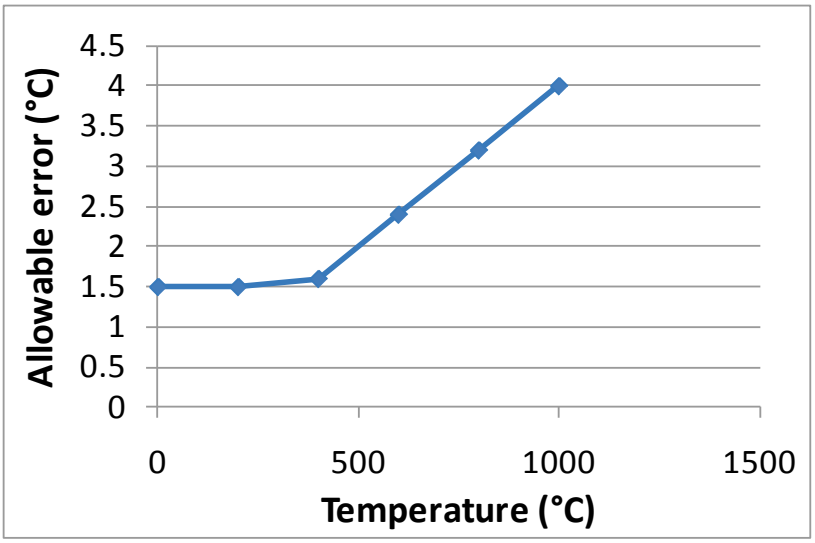

Figure A 1 Maximal error of temperature measurements of the type-K thermocouples used in the study.

Accuracy of measuring burning rate using thermocouple tree.

Measuring the burning rate with the thermocouple tree is associated with different errors. The error of the thermocouples as described above is almost irrelevant here since the difference in temperature between fuel surface and adjacent gas is very large. However, there are errors due to uneven spacing of the thermocouples and possible waves of the fuel surface.

The spacing of the thermocouples is measured using a ruler, thus errors will appear. Assuming that all errors combined such that the thermocouples from where we start the fit of burning rate to the end of the fit would be 1 mm too high at the top and 1 mm too low at the bottom. This would induce an additional 2 mm error over 60 mm. In addition, the spread of burning rate calculated from only two consecutive thermocouples is maximum 0.024 mm/ min. Consider that this is the error we obtain for all thermocouples that are used in the fit, and that the total time error is 20 seconds in the measurement over 60 mm. Combining these two errors of time and distance we get a burning time of 11.02 min over 62 mm instead of 11.32 min over 60 mm. This gives a total theoretical error of 8 %, a little more than the difference in burning rate measured between the two fuels.

However, from the small scale tests burning rate was measured both with the thermocouple tree and through the load cell system continuously recording the weight of the fuel. These two means of estimating burning rate showed good agreement with a maximum deviation of 5 % (E85).

Accuracy of the radiative heat flux measurements using plate thermometers and comparison with heat flux meters

The correlation between HFM and PT, without any smoothing can be seen in Figure A 2.

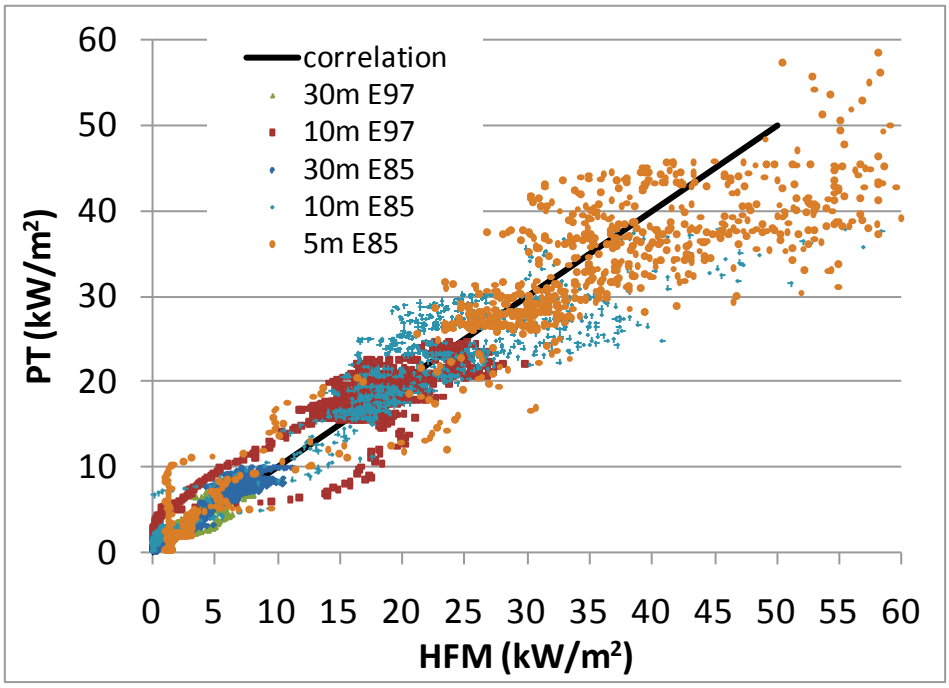

Figure A 2 Correlation of all data measured with traditional heat flux meters and the calculated heat flux based on the PT measurements.

Appendix 2 - Weather data

The weather data (temperature as well as wind speed and direction) was measured every minute during the test from a weather station 50 m from the pool centre and six meters from ground level. In the Figure A3 to A6 below, the wind direction is given as arrows displaying two minutes average direction. The temperature increased to over 50 °C for the E97 test. It should be remembered that this number is the temperature of the probe. If that is to be a representative of gas temperature the influence from convection must far exceed the influence from radiation. Gas temperatures are notoriously difficult to measure.

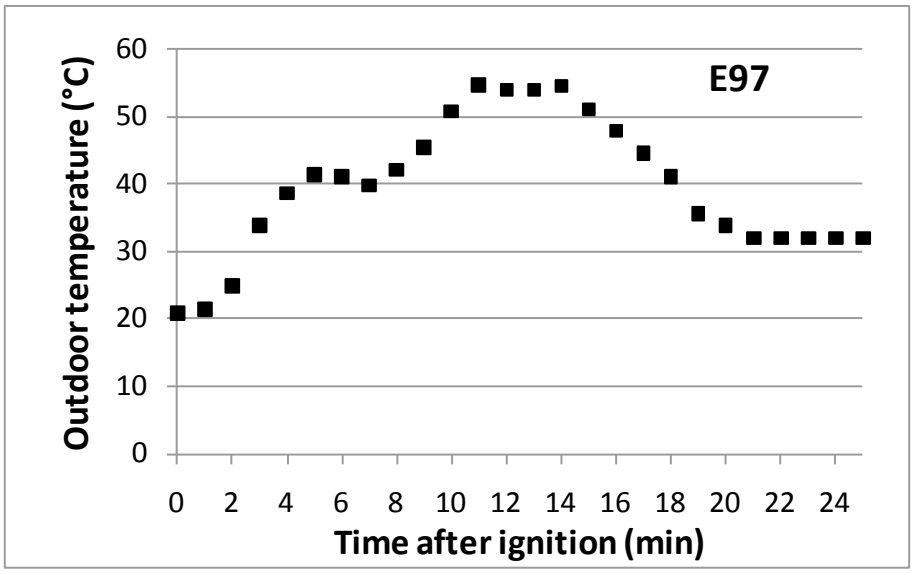

Figure A 3 Measured temperatures at the weather station during the E97 test.

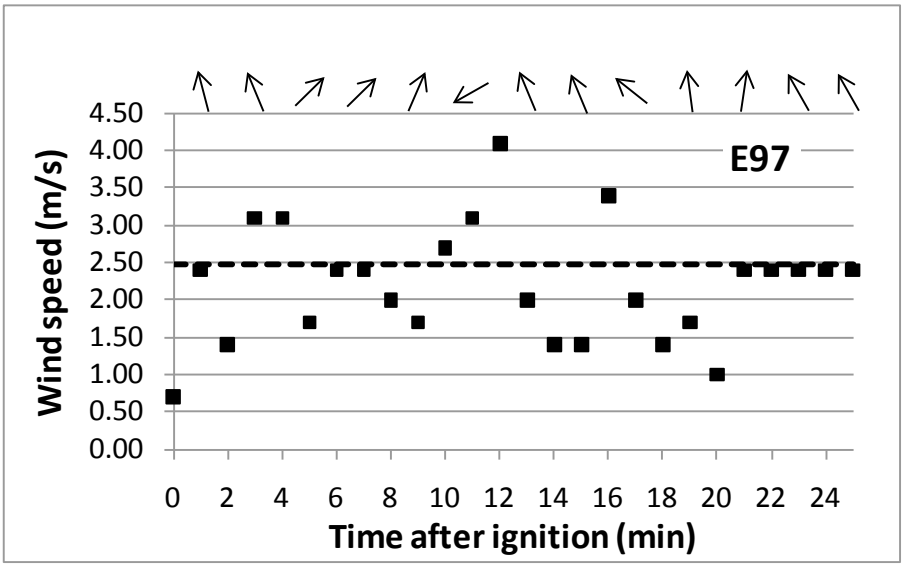

Figure A 4 Wind speed (one minute averages) and wind directions (two minutes averages) during the E97 test.

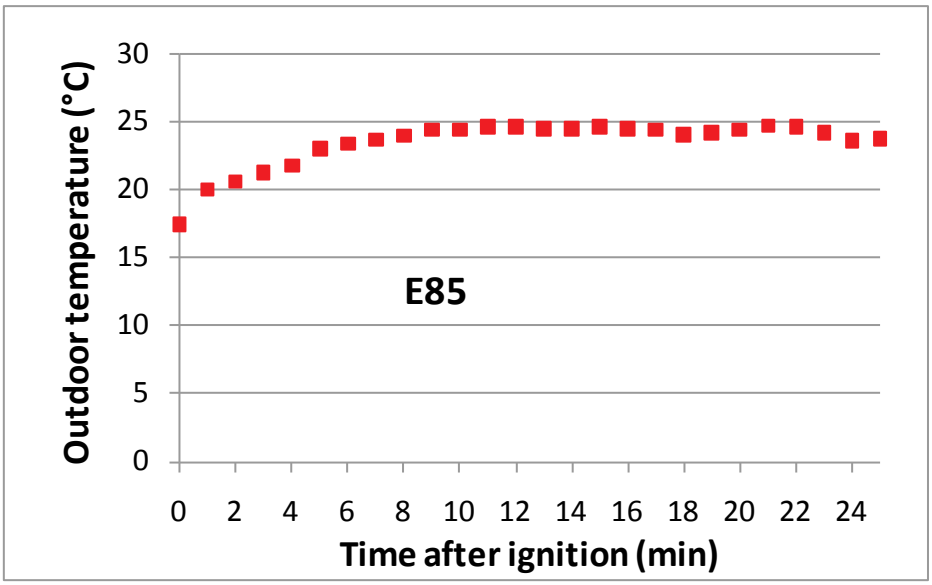

Figure A 5 Measured temperatures at the weather station during the E85 test.

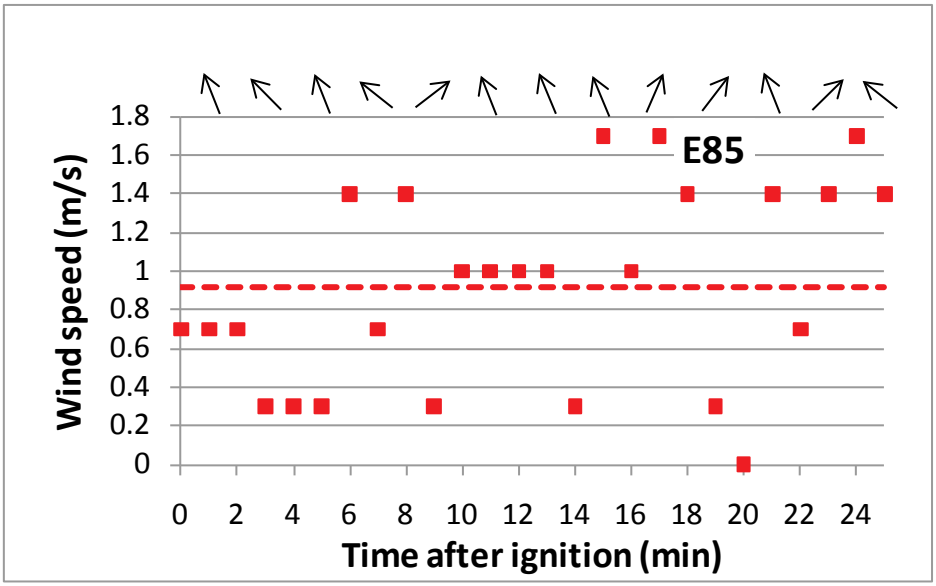

Figure A 6 Wind speed (one minute averages) and wind directions (two minutes averages) during the E85 test.

Appendix 3 – Observations and photos from the large scale tests

In this appendix, some photos are shown on the general test setup and from each of the large scale tests on E85 and E97. In addition, a short summary of the observations made during each test is also summarized.

In many photos, the bright light from the flame yield very dark areas from other parts of the photo suggesting that the smoke is darker that it actually was.

Figure A 7 The fuel filling pipe used during the tests and the support poles for the instrumentation in east direction.

Figure A 8 The instrumentation for burning rate and flame exposure in the center of the pool.

Figure A 9 The weather station located NW of the pool at about 4.5 m height above ground level.

Figure A 10 A view of the instrumentation in north (downwind) direction, including the elevated PT at 10 m distance from the rim of the pool.

Test 1-E97

The test was conducted 2012-08-28 and below is a summary of the visual observations made during the test and subsequent analysis of video recordings.

Time from ignition (min:s)	**Observations (made from video- and IR-camera positions, east direction)**
	13:30 - The truck started to fill up the pool with 20 000 L of E97 after some leakages had been repaired on the filling pipe.
	14:15 - Filling is completed
	14:23 - The filling pipe close to the pool is removed
	14:35 - Measurements are started (time 0:00 in data files) to provide background data and to allow control of all instrumentation
0:00	Fuel is ignited (measuring time 5:04)
0:15	The entire fuel surface is burning
1:00 (ca)	The heat exposure from the fire is clearly perceptible on exposed skin. Some smoke is visible above the flames. The flame height is about 1-1,5 times the pool diameter (D).
1:45 (ca)	Grass fire on the ground outside the outer concrete pool in north (downwind) direction.
2:15 (ca)	The grass fire is controlled/extinguished by fire personnel.
2:30 (ca)	Grass fire on the ground outside the outer concrete pool in northeast direction.
4:00 (ca)	Flame height estimated to be less than 1xD at some occasions. The heat exposure stings the skin in the face at about 50 m from the pool
4:30 (ca)	Small grass fire east of outer concrete pool
6:00 (ca)	At some occasions, the flame is narrow, almost perfect vertical and the top of the flame reach more than about 38 m (max height in video).
7:00 (ca)	The video camera has been zoomed out, max view about 46 m
7:45 (ca)	The tip of the flame reach almost 45 m at some few occasions
8:30 (ca)	The flames are leaning slightly more and the flame height is reduced
9:30 (ca)	The flame height is significantly lower than some minutes ago, effect of slightly increased wind, reduced burning rate?
11:10 (ca)	Almost no wind, the smoke is raising vertically. The smoke might have increased slightly.
12:20 (ca)	Small bangs from spalling of the concrete surface in the pool can be heard
12:45 (ca)	Intensive bangs from spalling of concrete
13:00 (ca)	The fire starts to self-extinguish along the rim of the pool
14:00 (ca)	Massive bangs from spalling of concrete, the flame height is reduced to less than 10 m. Smoke production increases.
15:00 (ca)	Only a a part of the pool surface is burning, flame height only some few meters.
16:00 (ca)	Only some few “islands” of burning fuel
18:30 (ca)	Fire only remaining in the drainage sump in the center of the pool
25:00	Measurements are terminated.

Figure A 11 A viewing of the fire plume from the south, 30 seconds after ignition of E97.

Figure A 12 A picture taken from south direction a few minutes after ignition of E97.

Figure A 13 A picture taken from west direction in the steady state phase of E97.

Figure A 14 A picture taken from northeast direction in the steady state phase of E97

Figure A 15 A picture of the fire plume towards the end of the E97 test.

Test 2-E85

The test was conducted 2012-08-29 and below is a summary of the visual observations made during the test and subsequent analysis of video recordings.

Time from ignition (min:s)	**Observations (made from video- and IR-camera positions, east direction)**
	10:55 - The truck started to fill up the pool with 20 000 L of 85
	11:55 - Filling is completed, the filling pipe close to the pool is removed
	12:08 - Measurements are started (time 0:00 in data files) to provide background data and to allow control of all instrumentation
0:00	Fuel is ignited (measuring time 5:00)
0:08	The entire fuel surface is burning
0:20 (ca)	The flame is more yellow/orange and produces significantly more smoke compared to the E97 fire. The flames are almost vertical and the flame height about 20-30 m but the higher parts of the flame is partly obscured by smoke.
2:15 (ca)	The flame height reaches up to 40 m occasionally. The most significant smoke plume starts at about 20 m height.
3:30 (ca)	The flame height reach about 47 m occasionally (max height in video).
4:00 (ca)	The video camera has been zoomed out, max view about 49 m. The heat exposure stings the skin in the face at about 50 m from the pool.
5:00 (ca)	There is no grass fire (already burnt) but occasionally, there is a lot of smoke along the ground due to the heat exposure.
6:00 (ca)	Wind has increased slightly, the flames are leaning and reach about 20-30 m.
7:00 (ca)	The flames are almost vertical again, flame height 30-40 m.
8:30 (ca)	Wind has increased slightly again and the flames are leaning.
9:30 (ca)	The flames are almost vertical again.
11:30 (ca)	The fire start to decline and the flame height is reduced. Bangs from spalling of concrete can be heard.
12:30 (ca)	Flame height about 10-15 m
12:40 (ca)	The fire is partly extinguished due to lack of fuel.
13:30 (ca)	Only a limited fire of about 5-10 m^2 in the center of the pool remaining. Smoke production increasing further.
14:15 (ca)	Remaining flames to a large extent obscured by smoke.
16:00 (ca)	Fire only remaining in the drainage sump in the center of the pool
25:00	Measurements are terminated.

Figure A 16 A view of the fire plume of E85 about 30 seconds after ignition, picture taken from the south.

Figure A 17 A view of the fire plume of E85 from northwest, a few minutes after ignition.

Figure A 18 A view of the smoke plume from E85. The picture was taken from northeast.

Figure A 19 A picture, taken from northeast, of the fire plume in the steady-state phase of E85.

Figure A 20 A picture, taken from northeast, of the fire plume in the steady-state phase of E85.

Figure A 21 Another picture of the smoke plume during the E85 test.

Figure A 22 A view of the fire plume from northwest at the end of the test with E85.

Figure A 23 A picture of the pool after the fire test

SP Technical Research Institute of Sweden

Our work is concentrated on innovation and the development of value-adding technology. Using Sweden's most extensive and advanced resources for technical evaluation, measurement technology, research and development, we make an important contribution to the competitiveness and sustainable development of industry. Research is carried out in close conjunction with universities and institutes of technology, to the benefit of a customer base of about 10000 organisations, ranging from start-up companies developing new technologies or new ideas to international groups.

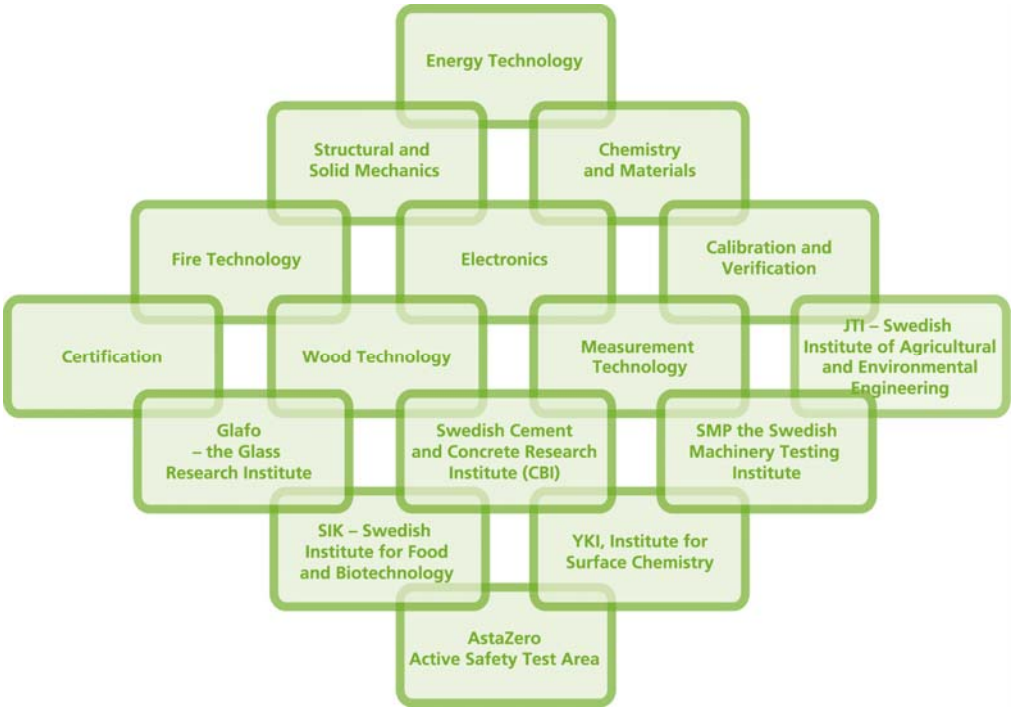

SP Technical Research Institute of Sweden
Box 857, SE-501 15 BORÅS, SWEDEN
Telephone: +46 10 516 50 00, Telefax: +46 33 13 55 02
E-mail: info@sp.se, Internet: www.sp.se
www.sp.se

Fire Technology
SP Report 2015:12
ISBN 978-91-88001-42-9
ISSN 0284-5172

More information about publications published by SP: **www.sp.se/publ**